Heavy Neutral Leptons During The Big Bang Nucleosynthesis Epoch

Instituut-Lorentz for Theoretical Physics
LEIDEN UNIVERSITY

Thesis submitted in partial fulfillment of
the requirements for the degree of

MASTER OF SCIENCE
in
PHYSICS

Author :	Nashwan Sabti
Student ID :	1367110
Supervisor :	Alexey Boyarsky
2nd corrector :	Ana Achúcarro

Leiden, The Netherlands, July, 2018

Heavy Neutral Leptons During The Big Bang Nucleosynthesis Epoch

Nashwan Sabti

Instituut-Lorentz, Leiden University
P.O. Box 9500, 2300 RA Leiden, The Netherlands

July, 2018

Abstract

Heavy Neutral Leptons are well-motivated candidates for explaining beyond Standard Model phenomena such as dark matter, baryon asymmetry of the Universe and neutrino oscillations. A variety of probes, ranging from collider-based to cosmological, explore regions of their parameter space in a complementary way. This work will delve into the possibility that Big Bang Nucleosynthesis has to offer in constraining their lifetime based on cosmological measurements of the Helium-4 abundance. Results are derived for masses up to 100 MeV and a framework is laid for extending the analysis to higher masses.

Table of Contents

CHAPTER 1

INTRODUCTION

1.1 Relevance of this work

A variety of cosmological, astrophysical and collider based probes can be used to put bounds on parameters of HNLs (Figure 1.1). Since the lifetime of an HNL is inversely proportional to the square of the mixing angle, a smaller mixing angle will lead to a longer lifetime, which means that such particles could be present at times relevant for BBN processes. An addition of HNLs to the Universe affects its cosmological expansion and the particle physics processes within compared to the standard case. Therefore, BBN provides a suitable probe for HNLs and gives a lower bound in the aforementioned parameter space.

Previous works [10–14, 17–19, 28] have studied the implications of HNLs on primordial nucleosynthesis for masses up to a couple hundreds of MeV. These results are then extrapolated to higher masses by assuming a certain maximum lifetime of HNLs and using the relation between mass, lifetime and mixing angle. In this way physical processes that may start to occur at higher masses are not taken into account, making the current bounds not so reliable. This work will review and revise the analysis of the effects of HNLs on BBN up to masses ~100 MeV and will provide a framework to extend this analysis to higher masses.

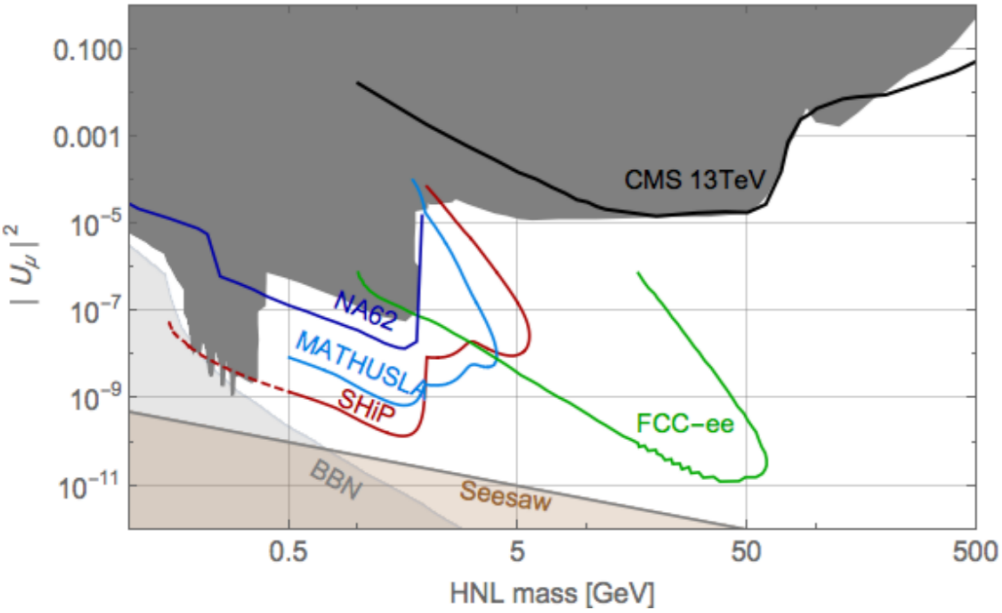

FIGURE 1.1: Current limits on the mixing between muon neutrino and a single HNL up to mass of 500 GeV. The brown region labeled 'Seesaw' corresponds to a naive estimate of the mixing scale in the canonical seesaw. The grey region labeled 'BBN' corresponds to an HNL lifetime >1 s, which is disfavored by BBN. Figure from [6].

1.2 Overview

This work will be more of a review that highlights the relevant points in this topic, rather than an extensive, repetitive study of what has come before. The interested reader is referred to [9] for a more deep dive into the subject of BBN.
Before jumping right into the new physics part, it is important to understand BBN within the framework of the Standard Model. Chapter 2 is dedicated to this. Chapter 3 introduces HNLs to the system and elaborates on some of their relevant properties. A brief description of the code that is used for simulating BBN together with some results are given in Chapter 4. The results are discussed in Chapter 5. Some technicalities will be expanded upon in the appendices.

CHAPTER 2

THE STANDARD CASE

The origin of primordial elements goes back to the early Universe. When going backwards in time, the Universe can be considered as a shrinking volume with increasing temperature. *Naively*, once this temperature exceeds the binding energy of a particle, be it element or hadron, it will be destroyed into its constituents. At some temperature one therefore expects a plasma of elementary particles that is in thermodynamic equilibrium. Now, going forward from this point in time, the Universe will be expanding and cooling down. This is the starting point of this chapter.

2.1 Defining the system

The main system is a plasma in an expanding universe. This system can be divided into two subsystems, based on the following processes:

- Cosmology & particle physics (denoted as *background* physics)
- Nuclear physics

Due to the smallness of the baryon-to-photon ratio, $\eta_{\mathrm{B}} \sim 10^{-10}$ [9], the influence of the second subsystem on the first one can be neglected; but not vice versa.

2.1.1 The background

At temperatures below QCD-scale, $T < \Lambda_{\rm QCD} \sim 150$ MeV [1], the dominant components of the background plasma are photons, charged leptons and active neutrinos, with here and there some traces of neutrons and protons. The expansion is governed by the energy density of the plasma and is described by the Friedmann equation

$$H^2 \equiv \left(\frac{\dot{a}}{a}\right)^2 = \frac{8\pi G}{3}\rho \,, \tag{2.1}$$

with H the Hubble parameter, a the scale factor and ρ the energy density.
In the case of radiation domination, this equation can be written as

$$H = \frac{1.66\sqrt{g_\star}}{M_{\rm pl}} T^2 \,, \tag{2.2}$$

with $g_\star$ the effective number of relativistic degrees of freedom and $M_{\rm pl}$ the Planck mass.
The background is assumed to be homogeneous and isotropic. The energy density ρ together with the total pressure P then satisfy the energy conservation law

$$\frac{{\rm d}\rho}{{\rm d}t} + 3H(\rho + P) = 0 \,. \tag{2.3}$$

While the Universe is expanding and cooling down, some species can get out of equilibrium (also known as *decoupling*). This happens at a temperature defined when the inequality

$$\Gamma(T) < H(T) \tag{2.4}$$

starts to hold. Here $\Gamma(T)$ is the rate of the reaction that keeps the particle in equilibrium. Relevant events during cooldown are [22]:

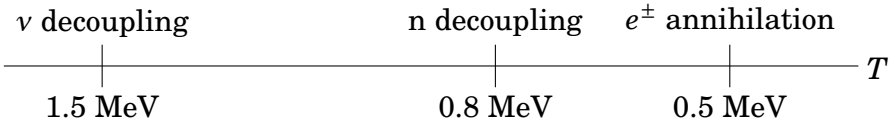

- Active neutrino thermal decoupling at $T \approx 1.5$ MeV.

- Baryon chemical decoupling at $T \approx 0.8$ MeV. This value is estimated by considering the reactions

$$n \leftrightarrow p + e^- + \bar{\nu}_e \tag{2.5}$$

$$n + \nu_e \leftrightarrow p + e^- \tag{2.6}$$

$$n + e^+ \leftrightarrow p + \bar{\nu}_e \tag{2.7}$$

- Electron-positron annihilation at $T \approx 0.5$ MeV.

Temperatures higher than Λ_{QCD} are not considered in the SM, since before neutrino decoupling the plasma is in equilibrium and nothing of importance for BBN happens.

2.1.2 Nuclei

Once neutrons decouple around $T \approx 0.8$ MeV, they will decay according to Eq. 2.5. This will go on until production of deuterium starts through the reaction

$$n + p \leftrightarrow D + \gamma \tag{2.8}$$

Due to the small baryon-to-photon ratio, the production of deuterium will not start at temperatures close to its binding energy $\Delta_D \approx 2.2$ MeV. Indeed, at such temperatures there are many photons with energies higher than Δ_D, which will destroy the deuterium nuclei immediately after they are created. This is also known as the *deuterium bottleneck*. Production of deuterium will become effective at temperatures much lower:

$$n_{\mathrm{baryons}} = \eta_{\mathrm{B}} n_\gamma = n_\gamma(E > \Delta_{\mathrm{D}}) \tag{2.9}$$

Solving this equation gives an estimate for the temperature of start of BBN, $T_{\mathrm{BBN}} \approx 70$ keV.

Once deuterium is formed, a series of nuclear reactions will lead to production of mainly ^{4}He. Heavier nuclei are produced in much smaller abundances, because

- there are no stable elements with mass number 5 and 8.

- the lack of sufficient densities of lighter nuclei diminishes the rates of nuclear reactions that produce heavier nuclei. Such processes are on the verge of decoupling around BBN temperatures.
- the Coulomb barrier causes electrostatic repulsion.

The last point is the main reason for decoupling of reactions involving heavier nuclei. Therefore, ^{4}He will be the most abundant element created during BBN, with here and there traces of heavier elements [9].

Following the previous discussion, the observables of BBN are abundances of light elements. In the Standard Model the only free parameter is the baryon-to-photon ratio η_{B} [9]. Thus, measuring this quantity (by abundance measurements or CMB measurements) leads to predictions of all primordial element abundances.

The most relevant abundance is that of ^{4}He, which can be described by the mass fraction $Y_{^4\mathrm{He}} = \frac{2\frac{n_n}{n_p}\big|_{T_{\mathrm{BBN}}}}{1+\frac{n_n}{n_p}\big|_{T_{\mathrm{BBN}}}}$. This quantity is determined by:

- Neutron-to-proton ratio $\frac{n_n}{n_p}$ at time of neutron decoupling. Using equilibrium physics:

$$\left.\frac{n_n}{n_p}\right|_{T_{\mathrm{ndec}}} = \frac{(m_n T_{\mathrm{ndec}})^{3/2} e^{-m_n/T_{\mathrm{ndec}}}}{(m_p T_{\mathrm{ndec}})^{3/2} e^{-m_p/T_{\mathrm{ndec}}}} \approx e^{-(m_n - m_p)/T_{\mathrm{ndec}}} \tag{2.10}$$

  T_{ndec} can be determined by equating the weak reaction rate in Fermi theory, $\Gamma \sim G_{\mathrm{F}}^2 T^5$, to the Hubble rate in Equation 2.2, which gives

$$T_{\mathrm{ndec}} \approx 0.8 \text{ MeV} \Rightarrow \frac{n_n}{n_p}(T_{\mathrm{ndec}}) \approx 0.16$$

- Time Δt between neutron decoupling and start of deuterium production. During this period neutrons will decay with mean lifetime τ:

$$\left.\frac{n_n}{n_p}\right|_{T_{\mathrm{BBN}}} \approx \frac{\left(\frac{n_n}{n_p}(T_{\mathrm{ndec}})\right) e^{-\Delta t/\tau}}{1 + \frac{n_n}{n_p}(T_{\mathrm{ndec}})\left[1 - e^{-\Delta t/\tau}\right]} \tag{2.11}$$

  Δt can be obtained from Equation 2.2, which gives $\Delta t \approx 150$ s. Plugging this in the equation above gives $\frac{n_n}{n_p}(T_{\mathrm{BBN}}) \approx 0.13$ and therefore $Y_{^4\mathrm{He}} \approx 0.23$.

Important quantities to keep in mind when studying BSM physics are therefore:

- Neutron-to-proton ratio at time of neutron decoupling.
- Hubble parameter H.

Chapter 4 will elaborate a little more on computations involving nuclei.

2.2 Regimes of particles

It is useful to categorize particles in the plasma in the following way:

- Massless & in-equilibrium (photons)
- Massive & in-equilibrium (charged leptons)
- Massless & out-of-equilibrium (active neutrinos)
- Massive & out-of-equilibrium (protons, neutrons and nuclei)

The first two groups of particles can be treated using equilibrium expressions. Using equilibrium physics for particles in the latter two groups gives incorrect abundances of heavy elements [20]. Instead, distributions of particles in the latter two groups are prone to distortions due to interactions around decoupling. These particles must therefore be treated properly within the framework of the Boltzmann equation.

2.3 Boltzmann equations in the SM

For the time being, only active neutrinos will be considered here. The baryons and nuclei will be dealt with in Chapter 4. Throughout this work no lepton asymmetry is assumed. At temperatures higher than the neutrino decoupling temperature, neutrinos will have a Fermi-Dirac distribution. At lower temperatures, a set of three Boltzmann equations must be solved [25]:

$$\frac{\mathrm{d}f_{\nu_\alpha}}{\mathrm{d}t} = H\frac{\mathrm{d}f_{\nu_\alpha}}{\mathrm{d}\ln a} = \sum_\beta I_\alpha P_{\beta\alpha} \ , \tag{2.12}$$

with $\alpha, \beta \in \{e, \mu, \tau\}$, $P_{\beta\alpha}$ time averaged transition probabilities and I_α the collision term, which encodes the details of interactions. The terms $P_{\beta\alpha}$ account for neutrino oscillations; more details and expressions are given in Appendix D. The collision term I_α for particle ν_α in the reaction

$$\nu_\alpha + 2 + 3 + ... + K \Longleftrightarrow (K+1) + (K+2) + ... + Q$$

has the general form [20]

$$I_\alpha = \frac{1}{2g_\alpha E_\alpha} \sum_{\text{in,out}} \int \prod_{i=2}^{Q} \frac{\mathrm{d}^3 p_i}{(2\pi)^3 2E_i} S |\mathscr{M}|^2 F[f] (2\pi)^4 \delta^4 (P_{\text{in}} - P_{\text{out}}) \,, \tag{2.13}$$

with g_α the degrees of freedom of ν_α, 'in' the initial states $\{\nu_\alpha, 2, ..., K\}$, 'out' the final states $\{(K+1), (K+2), ..., Q\}$, S the symmetry factor, $|\mathscr{M}|^2$ the *unaveraged*, squared matrix element summed over helicities of initial and final states and $F[f]$ the functional describing the particle population of the medium, given by

$$F[f] = (1 \pm f_{\nu_\alpha})...(1 \pm f_K) f_{K+1} ... f_Q - f_{\nu_\alpha} ... f_K (1 \pm f_{K+1}) ... (1 \pm f_Q) \,. \tag{2.14}$$

Here $(1 - f)$ is the Pauli blocking factor used for fermions and $(1 + f)$ the Bose enhancement factor used for bosons. The sum in Eq. 2.13 runs over all possible initial and final states involving ν_α.

2.4 Relevant interactions in the SM

All relevant reactions with active neutrinos should be considered:

- Neutrino pair annihilation into neutrino pair and neutrino-neutrino scattering: $\nu + \bar{\nu} \Leftrightarrow \nu + \bar{\nu}$ and $\nu + \nu \Leftrightarrow \nu + \nu$
- Neutrino-charged lepton scattering: $\nu + \ell^\pm \Leftrightarrow \nu + \ell^\pm$
- Neutrino pair annihilation into charged lepton pair and vice versa: $\nu + \nu \Leftrightarrow \ell^\pm + \ell^\mp$

All these reactions happen through charged current and neutral current weak interactions. Leading order diagrams at tree-level are given in Figure 2.1.

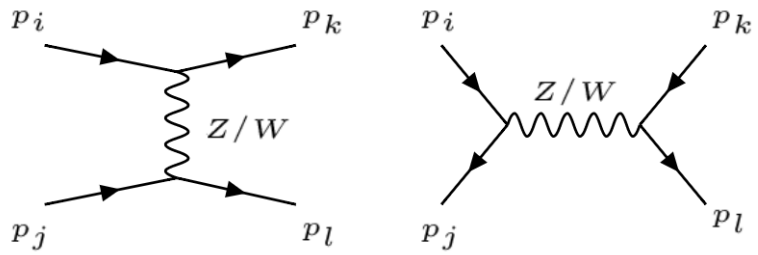

FIGURE 2.1: Leading order diagrams contributing to the collision integral in the Boltzmann equation for active neutrinos.

The squared matrix element in Fermi theory is of the following form for all reactions considered:

$$|\mathcal{M}|^2 = \sum_{i\neq j\neq k\neq l} \left[K_1(p_i\cdot p_j)(p_k\cdot p_l) + K_2 m_i m_j (p_k\cdot p_l)\right] , \tag{2.15}$$

with K_1, K_2 constants. Expressions for $|\mathcal{M}|^2$ of all relevant SM interactions involving active neutrinos are given in Table A.1. Since the baryon-to-photon ratio is very small, the assumption is made that Eqs. 2.5 - 2.7 do not alter the electron-neutrino distribution and are therefore neglected in the collision integral.

2.4.1 Four-particle collision integral

In the case of four-particle interactions, like

$$\nu_\alpha + 2 \Leftrightarrow 3 + 4$$

and similar crossing processes, the nine-dimensional collision integral can be reduced to a two-dimensional one. Using Eq. 2.15 in 2.13, the collision integral for a single reaction will be of the form

$$I_{\alpha,\text{single}} = \frac{1}{64\pi^3 g_\alpha E_\alpha p_\alpha} \int \mathrm{d}p_2 \mathrm{d}p_3 \frac{p_2 p_3}{E_2 E_3} SF[f] D(p_{\nu_\alpha}, p_2, p_3, p_4)\theta(E_4 - m_4) , \tag{2.16}$$

where the D-function is a conditional polynomial function of the four momenta p_{ν_α}, p_2, p_3 and p_4. The total collision term is then given by the sum of $I_{\alpha,\text{single}}$ for each reaction. The derivation of this equation is given in Appendix B.

2.5 Temperature evolution

The conservation of energy equation 2.3 can be used to derive an equation for the temperature evolution of the plasma. Using $\rho = \rho_{\mathrm{eq}} + \rho_{\mathrm{noneq}}$ (energy densities of particles in (non-)equilibrium) in Eq. 2.3 together with the fact that the temperature of the plasma is only defined for particles in equilibrium gives

$$\left(\frac{\mathrm{d}\rho_{\mathrm{eq}}}{\mathrm{d}T}\frac{\mathrm{d}T}{\mathrm{d}t} + \frac{\mathrm{d}\rho_{\mathrm{noneq}}}{\mathrm{d}t}\right) = -3H\left(\rho + P\right)$$

$$\frac{\mathrm{d}T}{\mathrm{d}t} = -\frac{3H(\rho + P) + \frac{\mathrm{d}\rho_{\mathrm{noneq}}}{\mathrm{d}t}}{\frac{\mathrm{d}\rho_{\mathrm{eq}}}{\mathrm{d}T}} \,. \tag{2.17}$$

Expressions for ρ_{eq} and ρ_{noneq} can be substituted in this equation to obtain an explicit formula for the temperature evolution. This is done in Appendix C.

2.6 System of equations

There are five equations that describe the primordial plasma and which have to be solved:

- Three Boltzmann equations for active neutrinos
- Friedmann equation
- Temperature evolution equation

These equations contain five unknowns - three active neutrino distribution functions $f_{\nu_\alpha}(t, p)$, scale factor $a(t)$ and temperature $T(t)$. Neutrinos and anti-neutrinos participate in similar reactions (charge conjugated channels for anti-neutrinos) and, since no lepton asymmetry is assumed, distribution functions of both are the same. Same principle holds for all other leptons. Initial distributions are taken as equilibrium distributions at time of decoupling. This system of equations is therefore closed and can be solved numerically.

CHAPTER 3

INTRODUCING HEAVY NEUTRAL LEPTONS

Over the last few years a plethora of extensions to the SM have been proposed to solve the yet unexplained observations of dark matter, baryon asymmetry of the Universe and neutrino masses. One of those ambitious extensions that aims to take down all of these problems at once is the νMSM. Introduced in [2, 3], this model adds three Heavy Neutral Leptons (HNLs) to the SM, making them the right-handed counterparts of active neutrinos. This chapter will explore the possibilities that BBN offers in constraining some of the parameters in this model.

3.1 The type I seesaw Lagrangian

The most general renormalizable Lagrangian that includes three right-handed neutrinos to the SM Lagrangian has the form [7]

$$\mathscr{L} = \mathscr{L}_{\mathrm{SM}} + i\overline{N}_I \partial_\mu \gamma^\mu N_I - \left(F_{\alpha I} \bar{L}_\alpha \widetilde{\phi} N_I + \frac{M_I}{2} \overline{N^c}_I N_I + \mathrm{h.c.} \right) , \tag{3.1}$$

with $I = \{1,2,3\}$, $\alpha = \{e,\mu,\tau\}$, N_I right-handed neutrinos (also known as HNLs or sterile neutrinos), $F_{\alpha I}$ Yukawa couplings, M_I HNL Majorana masses, L_α the SM lepton doublet and $\widetilde{\phi} \equiv i\sigma_2 \phi^*$ the conjugated Higgs doublet. Without loss of generality, the Majorana mass matrix can be chosen diagonal.
After electroweak symmetry breaking, the Dirac mass matrix can be defined as $(M_{\mathrm{D}})_{\alpha I} = \langle \phi \rangle F_{\alpha I} = \frac{v}{\sqrt{2}} F_{\alpha I}$, with $v = 246$ GeV.

The mass terms can then be rewritten as

$$\mathscr{L}_{\text{mass}} = -\frac{1}{2}\begin{pmatrix}\bar{\nu} & \overline{N^c}\end{pmatrix}\begin{pmatrix}0 & M_{\text{D}} \\ M_{\text{D}}^T & M_I\end{pmatrix}\begin{pmatrix}\nu^c \\ N\end{pmatrix} + \text{h.c.}\,, \tag{3.2}$$

where $N = (N_1\ N_2\ N_3)^T$, $\nu = \begin{pmatrix}\nu_e\ \nu_\mu\ \nu_\tau\end{pmatrix}^T$ and c indicates charge conjugation. Block-diagonalizing the mass matrix and assuming $M_{\text{D}} << M_I$ yields the type 1 seesaw formula

$$(M_\nu)_{\alpha\beta} = -\sum_I (M_{\text{D}})_{\alpha I} M_I^{-1} (M_{\text{D}}^T)_{I\beta}\,, \tag{3.3}$$

where M_ν is the 3×3 active neutrino mass matrix, which can be diagonalized by a unitary transformation with the PMNS-matrix V_{PMNS}. Defining the mixing angle matrix as

$$\theta_{\alpha I} \equiv (M_{\text{D}})_{\alpha I} M_I^{-1}\,, \tag{3.4}$$

the charge eigenstates ν and N in Eq. 3.2 can be written in terms of the mass eigenstates ν_{m} and N_{m} of the matrix $\text{diag}(V_{\text{PMNS}}^T M_\nu V_{\text{PMNS}}, M_I)$ up to leading order in θ:

$$\nu = V_{\text{PMNS}}\nu_{\text{m}} + \theta N_{\text{m}}^c \tag{3.5}$$

$$N = N_{\text{m}} - \theta^\dagger V_{\text{PMNS}}\nu_{\text{m}}^c\,. \tag{3.6}$$

The light mass eigenstates ν_{m} almost correspond to active neutrinos, while the heavy mass eigenstates N_{m} almost correspond to sterile neutrinos. The expression for ν can then be substituted in the weak interaction part of the SM Lagrangian, which gives the interaction of HNLs with SM particles:

$$\begin{aligned}\mathscr{L}_{\text{HNL,int}} = &-\frac{g}{4\cos\theta_{\text{W}}} Z_\mu \sum_I \sum_\alpha (\overline{N_{\text{m}}^c})_I \theta_{I\alpha}^* \gamma^\mu (1-\gamma_5)\nu_\alpha \\ &-\frac{g}{2\sqrt{2}} W_\mu^+ \sum_I \sum_\alpha (\overline{N_{\text{m}}^c})_I \theta_{I\alpha}^* \gamma^\mu (1-\gamma_5)\ell_\alpha^- + \text{h.c.}\end{aligned} \tag{3.7}$$

Therefore, HNLs couple to SM fields in a similar way as active neutrinos, but with an additional mixing angle that suppresses the interaction.

3.2 Properties of HNLs

For notational clarity, $(N_{\text{m}})_I$ is written as N_I, while keeping in mind that the latter is almost a charge eigenstate.

3.2.1 Roles of the individual HNLs

Among the three HNLs, N_1 serves as a dark matter candidate, which means it must be light, stable and very weakly interacting. In this scenario, the Yukawa coupling constants $F_{\alpha 1}$ in Eq. 3.1 are required to be very small. As a result, this particle gives a negligible contribution to the active neutrino mass matrix (Eq. 3.3) as well as the baryon asymmetry of the Universe [7]. Therefore, only N_2 and N_3 are responsible for these two phenomena and N_1 will be neglected from this point forward. In order to achieve successful baryogenesis, the masses of N_2 and N_3 are required to be close to degenerate.

3.2.2 Dirac spinor from two Majorana spinors

For the sake of convenience, both N_2 and N_3 are assumed to have the same mass M_N and same set of mixing angles $\{\theta_e, \theta_\mu, \theta_\tau\}$. Since both spinors are two-component Majorana spinors, it is possible to combine them into *one* Dirac spinor with four degrees of freedom. The HNL mass terms are approximately given by

$$\mathscr{L}_{\text{HNL,mass}} \approx -\frac{1}{2} M_N \left(\overline{N_2^c} N_2 + \overline{N_3^c} N_3 + \text{h.c.} \right) . \tag{3.8}$$

Constructing two Majorana spinors χ and ξ out of N_2 and N_3,

$$\chi = N_2^c + N_2 \tag{3.9}$$

$$\xi = N_3^c + N_3 , \tag{3.10}$$

and substituting this in Eq. 3.8 gives

$$\mathscr{L}_{\text{HNL,mass}} = -\frac{1}{2} M_N \left(\bar{\chi}\chi + \bar{\xi}\xi \right) . \tag{3.11}$$

Define the Dirac spinor as

$$N_{\text{D}} = \frac{1}{\sqrt{2}} \left(\chi + i\xi \right) \tag{3.12}$$

$$N_{\text{D}}^c = \frac{1}{\sqrt{2}} \left(\chi - i\xi \right) \tag{3.13}$$

and Eq. 3.11 becomes

$$\mathscr{L}_{\text{HNL,mass}} = -\frac{1}{2} M_N \left(\overline{N_{\text{D}}} N_{\text{D}} + \overline{N_{\text{D}}^c} N_{\text{D}}^c \right) = -M_N \overline{N_{\text{D}}} N_{\text{D}} . \tag{3.14}$$

Therefore, from this point on, a Dirac particle (and its charge conjugate) with two degrees of freedom, mass M_N and three mixing angles θ_α will be considered.

3.2.3 Shortcut for calculation matrix elements of HNLs

Expressions for N_I^c in terms of N_{D} and N_{D}^c,

$$N_2 + N_2^c = \frac{1}{\sqrt{2}}\left(N_{\mathrm{D}} + N_{\mathrm{D}}^c\right) \tag{3.15}$$

$$N_3 + N_3^c = \frac{1}{i\sqrt{2}}\left(N_{\mathrm{D}} - N_{\mathrm{D}}^c\right) \ , \tag{3.16}$$

together with $\theta_{2\alpha} = \theta_{3\alpha} = \theta_\alpha$ can be substituted in Eq. 3.7 to give

$$\begin{aligned}
\mathscr{L}_{\mathrm{HNL,int}} =& -\frac{g}{4\cos\theta_{\mathrm{W}}} Z_\mu \sum_\alpha \frac{1}{\sqrt{2}} (\overline{N_{\mathrm{D}} + N_{\mathrm{D}}^c - iN_{\mathrm{D}} + iN_{\mathrm{D}}^c}) \theta_\alpha^* \gamma^\mu (1-\gamma_5) \nu_\alpha \\
& - \frac{g}{2\sqrt{2}} W_\mu^+ \sum_\alpha \frac{1}{\sqrt{2}} (\overline{N_{\mathrm{D}} + N_{\mathrm{D}}^c - iN_{\mathrm{D}} + iN_{\mathrm{D}}^c})_I \theta_\alpha^* \gamma^\mu (1-\gamma_5) \ell_\alpha^- + \mathrm{h.c.} \\
=& -\frac{g}{4\cos\theta_{\mathrm{W}}} Z_\mu \sum_\alpha (\overline{e^{-i\frac{\pi}{4}} N_{\mathrm{D}} + e^{i\frac{\pi}{4}} N_{\mathrm{D}}^c}) \theta_\alpha^* \gamma^\mu (1-\gamma_5) \nu_\alpha \\
& - \frac{g}{2\sqrt{2}} W_\mu^+ \sum_\alpha (\overline{e^{-i\frac{\pi}{4}} N_{\mathrm{D}} + e^{i\frac{\pi}{4}} N_{\mathrm{D}}^c})_I \theta_\alpha^* \gamma^\mu (1-\gamma_5) \ell_\alpha^- + \mathrm{h.c.} \\
=& -\frac{g}{4\cos\theta_{\mathrm{W}}} Z_\mu \sum_\alpha (\overline{N_{\mathrm{D}} + N_{\mathrm{D}}^c}) \theta_\alpha^* \gamma^\mu (1-\gamma_5) \nu_\alpha \\
& - \frac{g}{2\sqrt{2}} W_\mu^+ \sum_\alpha (\overline{N_{\mathrm{D}} + N_{\mathrm{D}}^c})_I \theta_\alpha^* \gamma^\mu (1-\gamma_5) \ell_\alpha^- + \mathrm{h.c.} \ ,
\end{aligned} \tag{3.17}$$

where the $e^{\pm i\frac{\pi}{4}}$ are absorbed in the N_D fields. It can be seen now that the characteristics of the Majorana particles have not disappeared: particle and its charge conjugate still interact in the same way. Since no lepton asymmetry is assumed, both particle and its charge conjugate can be treated on an equal footing. Therefore, it is enough to compute only one matrix element, which can be obtained by

$$|\mathscr{M}|_N^2 = |\theta_\alpha|^2 \, |\mathscr{M}|_\nu^2 \tag{3.18}$$

The effect of the charge conjugated particle is then taken into account through the degrees of freedom. As long as the Dirac particle has the same lifetime, mixing pattern and spectrum as the Majorana particle, the two cases are equivalent.

3.2.4 Decoupling temperature

An initial condition must be provided when solving the Boltzmann equation. This is chosen as the Fermi-Dirac distribution at a temperature little higher than HNL decoupling temperature.

A naive approach for determining the decoupling temperature is to equate the weak interaction rate in Fermi theory in the ultra-relativistic limit to the Hubble rate for a radiation dominated universe:

$$\frac{1.66\sqrt{g_*}}{M_{\mathrm{pl}}}T^2 = \theta_{\mathrm{M}}^2(T)G_{\mathrm{F}}^2T^5 \ , \tag{3.19}$$

where $\theta_{\mathrm{M}}(T)$ is the effective mixing angle in a medium, which arises from a self-energy term induced by interactions of active neutrinos with particles in the medium. An explicit expression is given by [5, 7, 23]

$$\theta_{\mathrm{M}}^2(T) = \frac{\theta^2}{\left(1+\frac{2p}{M_N^2}\left(\frac{16G_{\mathrm{F}}^2}{\alpha_{\mathrm{W}}}p\left(2+\cos^2\theta_{\mathrm{W}}\right)\frac{7\pi T^4}{360}\right)\right)^2+\theta^2} \ , \tag{3.20}$$

with θ the mixing angle in vacuum and α_{W} the weak coupling constant. Plugging $\theta^2 = 10^{-6}$, $g_* = 20$ and $p \sim \pi T$ in Eq. 3.19 yields a decoupling temperature of $T_{\mathrm{dec}} \sim 160$ MeV for $M_N \sim 100$ MeV. For higher masses or larger mixing angles this approach becomes less credible, because at some point the HNLs will decouple non-relativistically.

More sophisticated approaches have been developed in [15, 16, 27] and found decoupling temperatures of $\mathcal{O}(1)$ GeV for masses $0.5 \leq M_N \leq 1$ GeV. It has been shown in [15] that HNLs with such masses will always enter equilibrium at temperatures above $T \sim 5$ GeV.
This work will use these results as a guide by looking at what temperatures the distribution function will start to differ from the equilibrium one. This transition point should give an estimation for the decoupling temperature.

3.2.5 Dependence of mixing angle on temperature

As can be seen in the previous subsection, the mixing angle θ_{M} depends on the temperature of the medium. However, it can be shown that θ_{M} differs from θ as [25]

$$\frac{\theta_{\mathrm{M}}-\theta}{\theta} \sim \frac{G_{\mathrm{F}}T^6}{M_{\mathrm{W}}^2M_N^2} \sim 10^{-11}\left(\frac{T}{100\ \mathrm{MeV}}\right)^6\left(\frac{10\ \mathrm{MeV}}{M_N}\right)^2 \ , \tag{3.21}$$

which means that for temperatures relevant for BBN, $T \sim 1$ MeV, and masses of interest, up to $M_N \sim 1$ GeV, the mixing angle is not altered significantly in the plasma and medium effects are negligible.

3.2.6 Contribution to energy density of the Universe

The inclusion of an HNL to the background described in subsection 2.1.1 has consequences for its expansion. Assuming the HNL decouples non-relativistically, its energy density at temperatures $T < T_{\text{dec}} < T_{\text{NR}} \sim M$ is given by

$$\begin{aligned}\rho_N(T) &\sim M_N n_N(T_{\text{dec}})\left(\frac{a_{\text{dec}}}{a}\right)^3 \sim M_N n_N(T_{\text{dec}})\frac{g_*(T)T^3}{g_*(T_{\text{dec}})T_{\text{dec}}^3} \\ &\sim 4\left(\frac{M_N T_{\text{dec}}}{2\pi}\right)^{\frac{3}{2}} e^{-M_N/T_{\text{dec}}}\frac{g_*(T)T^3}{g_*(T_{\text{dec}})T_{\text{dec}}^3}\,,\end{aligned} \tag{3.22}$$

where entropy conservation, $g_*(T_1)a_1^3T_1^3 = g_*(T_2)a_2^3T_2^3$, is used. Equating this density to the energy density of radiation gives

$$4\left(\frac{M_N T_{\text{dec}}}{2\pi}\right)^{\frac{3}{2}} e^{-M_N/T_{\text{dec}}}\frac{g_*(T)T^3}{g_*(T_{\text{dec}})T_{\text{dec}}^3} = g_*(T)\frac{\pi^2}{30}T^4 \Longrightarrow T \sim 30\text{ keV} \tag{3.23}$$

for $M_N \sim 50$ MeV, $\theta^2 \sim 10^{-4}$, $T_{\text{dec}} \sim 30$ MeV and $g_*(T_{\text{dec}}) \sim 10$.

This means that the Universe will become matter dominated at the time nuclear reactions are taking place. Therefore, if the HNL has not decayed yet long before this time, it could have a direct impact on the abundances of primordial elements.

3.2.7 Contribution to temperature evolution

The HNL here belongs in the category 'massive and out-of-equilibrium' and will only add a term to the numerator in Eq. 2.17. An interpretation of this term is that interactions involving HNLs will lead to final particle states that have higher energies than those in the plasma. Only final particle states that equilibrate with the plasma will heat up the background. This means that, e.g., active neutrinos coming from decay of HNLs will not contribute to the temperature evolution after neutrino decoupling.

3.3 Relevant interactions of HNLs

All interactions of HNLs with SM particles are mediated by charged and neutral currents. The higher the mass, the more channels will be available. All relevant interactions together with the corresponding matrix elements for HNL masses up to ~ 1 GeV are summarized in A.2 and A.3.

Since HNLs can decouple at temperatures higher than $\Lambda_{\mathrm{QCD}} \sim 150$ MeV, interactions above and below this border must be distinguished.

3.3.1 Interactions above QCD-scale

At temperatures $T > \Lambda_{\mathrm{QCD}}$ no bound states of quarks exist and only two types of reactions should be considered:

- Interactions with active neutrinos and charged leptons.
- Interactions with free quarks. Here, only interactions with two quarks are considered, since multiquark final states are suppressed by higher orders of the coupling α_s in perturbative QCD [8].

Contributing diagrams are of the following form:

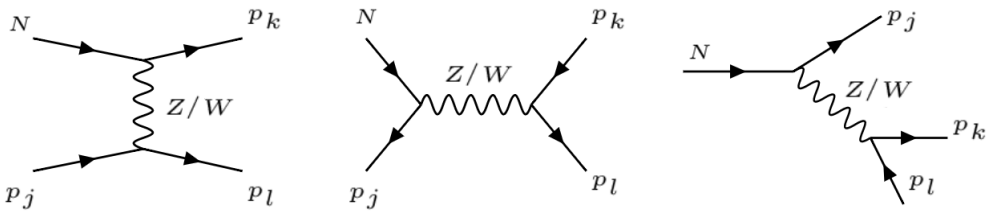

FIGURE 3.1: Leading order diagrams contributing to the collision integral in the Boltzmann equation for an HNL at temperatures $T > \Lambda_{\mathrm{QCD}}$.

3.3.2 Interactions below QCD-scale

At temperatures $T < \Lambda_{\mathrm{QCD}}$ quarks are confined within bounds states. All reactions in the previous section are four-particle interactions. In this case three- and four-

particle interactions are considered:

- Interactions with active neutrinos and charged leptons like before.
- Interactions with a single meson in the final state. Only HNL decays are considered here, since the creation of a meson h in the reaction $N + \nu/\ell \to h$ is only possible when $M_N < M_h$. Moreover, at temperatures of $\mathcal{O}(1)$ MeV the rate of this reaction is much smaller than the decay rate of HNLs. The only contributing diagram is therefore:

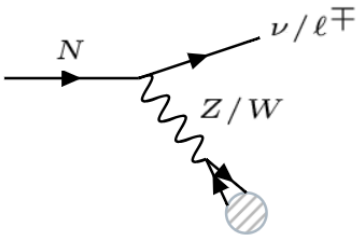

FIGURE 3.2: Leading order diagram for three-particle reactions contributing to the collision integral in the Boltzmann equation for an HNL at temperatures $T < \Lambda_{\mathrm{QCD}}$.

The branching ratios of the relevant HNL decay channels are plotted in Figure 3.3.

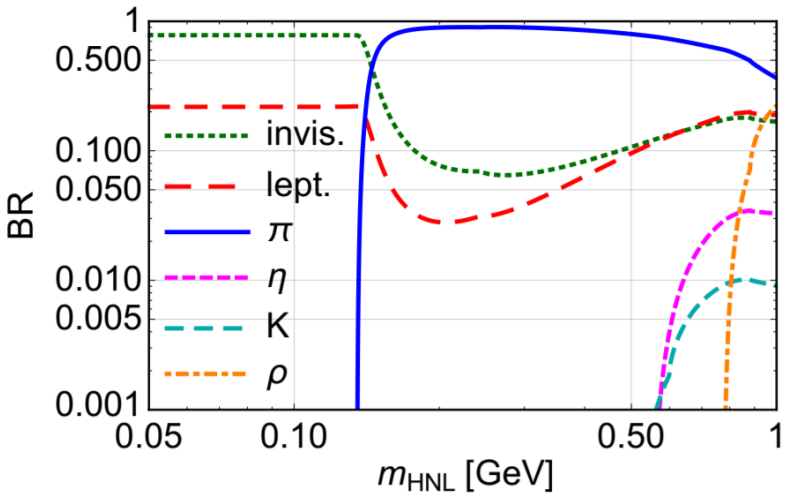

FIGURE 3.3: The branching ratios of relevant HNL decay channels. Figure from [6].

Interactions with more than two mesons in the final state are not considered, except for reactions with two pions in the final states, such as $N \to \nu + \pi^+ + \pi^-$. These reactions are taken into account by resonance of ρ meson, i.e., $N \to \nu + \rho^0 \to \nu + \pi^+ + \pi^-$. It has been shown in [6] that the decay width of both two reactions coincide and, therefore, decay into two pions happens predominantly via decay into ρ meson. The decay channel to two pions is also open for $2m_\pi < M_N < m_\rho$, but this contribution is negligible.

The contribution of decays into multi-meson final states to the full hadronic decay width can be estimated by comparing the combined decay width of single-meson final states with the full hadronic decay width. The full hadronic decay width can be estimated by considering the total decay width into quarks. The result can be seen in Figure 3.4. Multi-meson final states become important for masses $M_N > 1$ GeV, while for masses smaller it is enough to consider only single-meson channels as the hadronic decay modes.

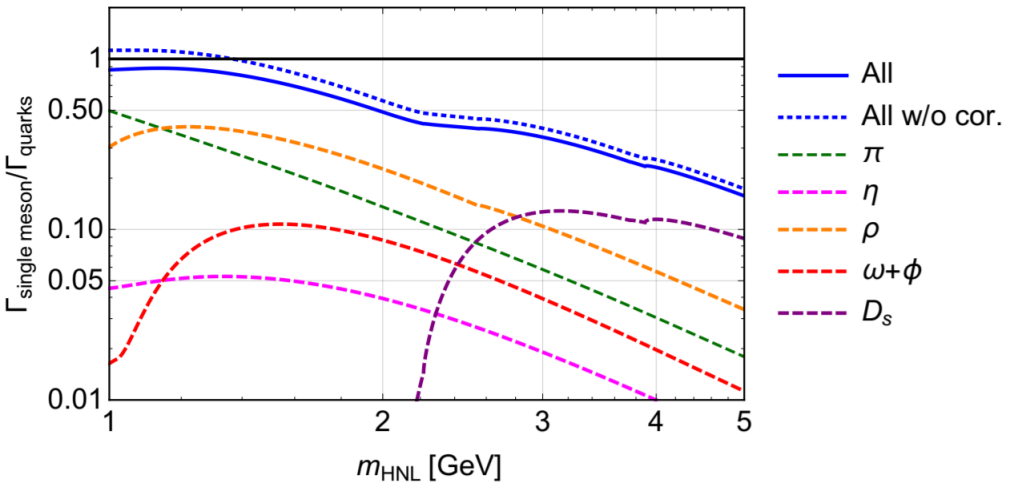

FIGURE 3.4: HNL decay widths of channels with single meson final states divided by the total decay width into quarks with QCD corrections (dashed lines). The two blue lines are the sum of these ratios, where QCD corrections were (solid line) and were not (dotted line) applied to the total decay width into quarks when computing the ratios. Figure from [6].

3.3.3 Interactions of unstable decay products with plasma

HNLs with masses $M_N < 105$ MeV will decay into stable particles. HNLs with higher masses will have decay products that are unstable. Some of these unstable decay products will interact with the plasma before they decay. The analysis here will be done for muons, but can be applied to all other particles as well.
There are three important events to consider:

1. $\mu^{\pm}$ is created from HNL decay
   The distribution function of these muons is a non-thermal distribution f_{noneq}.

2. $\mu^{\pm}$ thermalizes
   The muon-photon scattering rate is higher than the muon decay rate:
   $\Gamma_{\gamma\mu} \sim \frac{\alpha^2}{m_\mu E_\gamma} T_\gamma^3 \sim 10^{-9}$ MeV vs. $\Gamma_{\mu,\text{decay}} \sim 10^{-16}$ MeV. This means that the muons will release their energy into the plasma and equilibrate before they decay. This process increases the temperature of the plasma and makes the muons non-relativistic. After thermalization the muons will share the same temperature as the plasma and will have a thermal distribution
   $f_{\text{thermal}} = e^{-\frac{m_\mu - \mu}{T}} e^{-\frac{p^2}{2m_\mu T}}$, where μ is determined by the condition that the number density before and after thermalization must be equal. The collision term corresponding to this process is then estimated as

   $$I_{\text{thermalization}} \approx \frac{f_{\text{thermal}} - f_{\text{noneq}}}{\Delta t} ,$$

   with Δt the timestep of the simulation. The same procedure is followed for charged pions and charged kaons.

3. $\mu^{\pm}$ decays
   The main decay channel of muons is $\mu^- \to e^- + \overline{\nu_e} + \nu_\mu$. The muon has a lifetime, $\tau_\mu \sim 10^{-6}$ sec., that is much smaller than the timestep of the simulation. This poses a problem right away: when the evolution of the distribution function for the muon and active neutrinos is computed as $\Delta f = I_{\text{coll}} \Delta t$, the behaviour of I_{coll} is not resolved. It is assumed to be constant during the whole timestep Δt, which is not true; the created muons have already decayed well within this timestep. What therefore happens is that the amount of muons that have decayed and the amount of neutrinos that are created, are overestimated.

This issue can be solved by using dynamical equilibrium. Consider the chain

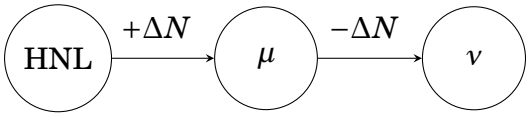

The timestep Δt is much smaller than the lifetime of the HNL, which means that there is approximately a constant inflow of muons *during* each timestep. Since the amount of muons created ΔN decays almost instantaneously, the same number of active neutrinos is created: for each muon that decays, one electron neutrino and one muon neutrino is created. Now a scaling α can be introduced in $\Delta f = I_{\text{coll}} \Delta t \alpha$ such that $\int \mathrm{d}^3 p \Delta f/(2\pi)^3 = \Delta N$.

3.4 Boltzmann equation for HNLs

In this model, one more equation must be added to the system of equations in Section 2.6. At temperatures below the HNL decoupling temperature, the HNL distribution function f_N can be obtained by solving the Boltzmann equation

$$\frac{\mathrm{d}f_N}{\mathrm{d}t} = I_N \,, \tag{3.24}$$

with I_N the collision term. Besides the four-particle collision integral in Eq. 2.16 there is also a three-particle collision integral.

3.4.1 Three-particle collision integral

In the case of a two-body decay

$$N \to 2 + 3 \,, \tag{3.25}$$

the six-dimensional collision integral in Eq. 2.13 can be reduced to a one-dimensional integral. Since the matrix element for three-particle interactions does not depend on the four-momenta of the particles, it has the simple form

$$I_{N,\text{single}} = \frac{\pi S |\mathscr{M}|^2}{4 g_N E_N p_N} \int \mathrm{d}p_2 \frac{p_2}{E_2} F(f) \mathscr{X} \theta \left((\widetilde{E_N} - \widetilde{E_2})^2 - \frac{x^2}{M^2} m_3^2 \right) \tag{3.26}$$

for each reaction taken into account. Here, $\mathscr{X}$ is given by

$$\mathscr{X} = \frac{\pi}{8} (-\mathrm{Sgn}[p_1 - p_2 - p_3] + \mathrm{Sgn}[p_1 + p_2 - p_3] + \mathrm{Sgn}[p_1 - p_2 + p_3] - 1) \,, \tag{3.27}$$

with Sgn the Signum function.

3.5 Influence of HNLs on BBN

Subsection 2.1.2 listed the two main points that determine the course of BBN. If HNLs decay before neutrino decoupling, the plasma will just re-equilibrate and nothing will change. But if decay happens after neutrino decoupling, then HNLs can influence BBN by

- their contribution to the cosmological energy density.
  An increase in the energy density leads to a higher expansion rate according to the Friedmann equation 2.1. The decoupling temperature of weak interactions, determined by $H = \Gamma \sim T_{\mathrm{dec}}^5$, will then be higher compared to the standard case. Therefore, the $\frac{n_{\mathrm{n}}}{n_{\mathrm{p}}}$−ratio at time of neutron decoupling, Eq. 2.10, will be larger. This will lead to a larger helium mass fraction $Y_{^4\mathrm{He}}$.

- their decay products.
  HNL decay injects active neutrinos and electrons/positrons into the plasma with energies that may be different from typical energies of plasma particles.

  – Decay into ν_μ and ν_τ will increase the expansion rate with respect to the standard case and this will therefore increase the $\frac{n_{\mathrm{n}}}{n_{\mathrm{p}}}$−ratio at neutron decoupling and thus increase $Y_{^4\mathrm{He}}$.

  – Decay into ν_e has two effects: (I) it will increase the expansion rate similarly to above and (II) it will preserve equilibrium between neutrons and protons for a longer time, since they participate in the reactions in Eqs. 2.5 - 2.7. The latter effect would make the $\frac{n_{\mathrm{n}}}{n_{\mathrm{p}}}$−ratio at neutron decoupling smaller. Effect (II) is stronger than (I) [10] and the net effect will be a decrease of $Y_{^4\mathrm{He}}$.

  – Decay into $e^\pm$ will inject more energy into electromagnetic part of the plasma and heat it up, which increases the expansion rate and increases $Y_{^4\mathrm{He}}$.

The net effect is of course an interplay between all above mentioned effects, each of which is influenced by the HNL mass and mixing pattern. BBN will therefore provide a lower bound on the mixing angles or, equivalently, an upper bound on the lifetime.

CHAPTER 4

RESULTS

This chapter will present results for neutrino decoupling spectra in the SM and bounds on HNL lifetime as a function of its mass. The latter is done for HNL masses up to $M_N = 100$ MeV where mixing with only electron neutrino is turned on. The bounds are obtained by comparing the ^{4}He mass fraction obtained from simulations with measurements done in [4].

4.1 Simulating BBN with PYBBN

The computational scheme of the code (PYBBN) used to do the simulations will be briefly summarized here. An extensive user guide with schemes, approximations, results and comparisons with literature will be available soon on the homepage[1] of the code.

Simulations are done in two steps: (I) The background physics and the rates of the reactions in Eqs. 2.5 - 2.7 are computed in PYBBN. This involves solving the system of equations in Section 2.6 for the evolution of temperature, scale factor and distribution functions of decoupled species. (II) The cosmological quantities

[1] https://github.com/ckald/pyBBN

together with the aforementioned rates are tabulated and passed to an external code, the modified KAWANO code [25], that takes care of the nuclear part of the simulation and outputs the light element abundances.
The ^{4}He abundance can then be compared with what is determined by [4] as

$$Y_{^4\mathrm{He}} = 0.2452 - 0.2696 \qquad (2\sigma \text{ interval}) \tag{4.1}$$

4.2 Results for Standard Model BBN

The temperature evolution is the first interesting point to consider, since it will show the heat up of the plasma due to electron-positron annihilation. The result is shown in Figure 4.1.

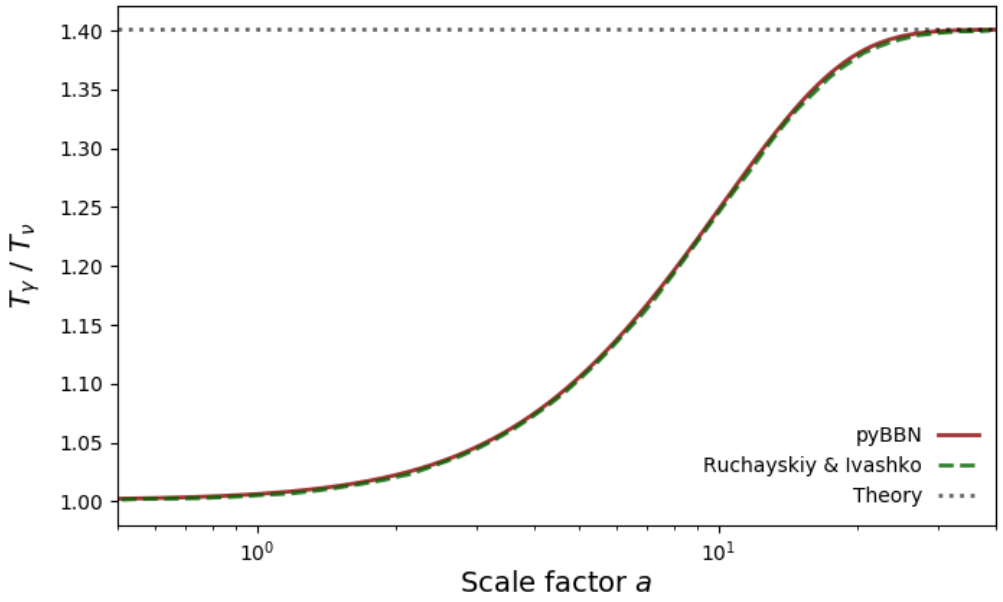

FIGURE 4.1: The photon temperature divided by active neutrino temperature. The increase here is due to electron-positron annihilation into photons. Dashed curve is from [25].

The theoretical value is obtained by using entropy conservation:

$$\frac{T_\gamma}{T_\nu} = \frac{aT_\gamma}{aT_\nu} = \left(\frac{g_*(T_{\text{before}})}{g_*(T_{\text{after}})}\right)^{\frac{1}{3}} = \left(\frac{\frac{7}{8}\cdot 4 + 2}{2}\right)^{\frac{1}{3}} \approx 1.401 \tag{4.2}$$

The next step is to compare the active neutrino spectra at the end of electron-positron annihilation with their equilibrium distribution at high temperature. The result is shown in Figure 4.2.

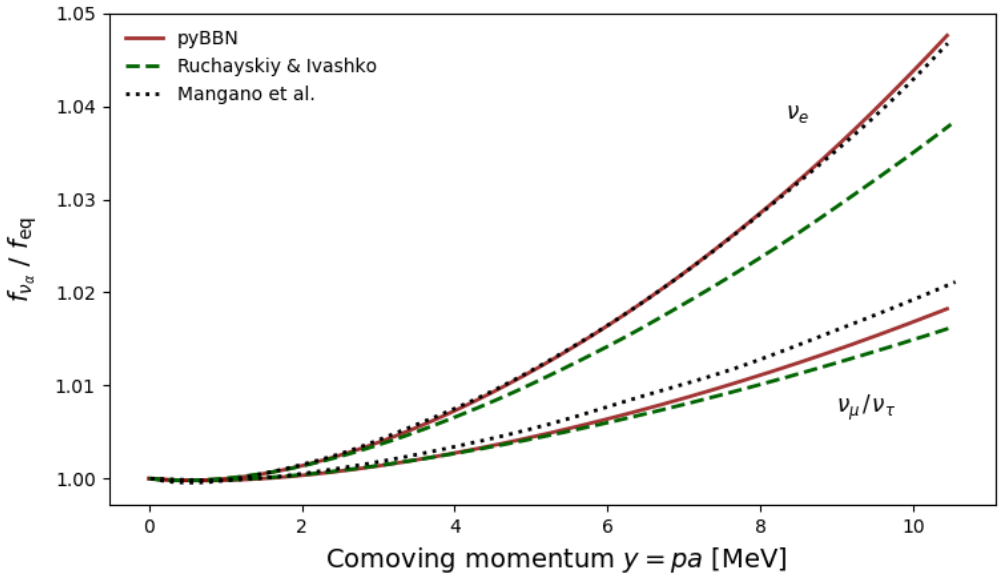

FIGURE 4.2: Ratio of active neutrino decoupled spectra to their equilibrium distribution before the onset of BBN. The upper curves show the distortion of the electron neutrino spectrum and the lower of muon and tau neutrinos. Neutrino flavour oscillations are not taken into account here. Dashed curves are from [25], dotted from [21].

In Fermi theory the cross section increases with momentum as $\sigma \propto G_F^2 p^2$, which means that neutrinos with higher momenta stay longer in equilibrium. Since these neutrinos decouple later, they will briefly experience the heat-up of the plasma due to electron-positron annihilation, shown in Figure 4.1, and the corresponding increase in aT. Their equilibrium distribution function, given by

$$f_\nu = \frac{1}{e^{\frac{p}{T}} + 1} = \frac{1}{e^{\frac{y}{aT}} + 1} \,,$$

increases then accordingly.

At temperatures of $\mathcal{O}(1)$ MeV electron neutrinos interact through both charged and neutral current, while muon and tau neutrinos only interact through neutral current. The temperature is too low for muons and tau leptons to be present in the

plasma or to be created from muon and tau neutrinos. The cross section of electron neutrinos is therefore larger and they stay longer in equilibrium.
When the relevant cosmological quantities are passed to the modified KAWANO code, a value of $Y_{^4\mathrm{He}} = 0.24793$ is obtained; in agreement with the result in Eq. 4.1.

4.3 Results for νMSM

Results are shown here for HNLs with masses up to 100 MeV that mix with electron neutrino only. There are four channels through which the HNL can decay,

$$N \to \nu_e + \nu_e + \overline{\nu_e} \qquad N \to \nu_e + \nu_\mu + \overline{\nu_\mu}$$
$$N \to \nu_e + \nu_\tau + \overline{\nu_\tau} \qquad N \to \nu_e + e^+ + e^- \ ,$$

and from which the lifetime can be computed as

$$\tau_N = \Gamma_N^{-1} = \frac{192\pi^3}{G_F^2 |\theta_e|^2 M_N^5 \left(\frac{1}{4}\left(1 + 4\sin^2\theta_W + 8\sin^4\theta_W\right) + 1\right)} \tag{4.3}$$

This equation is used to obtain the plot in Figure 4.3.

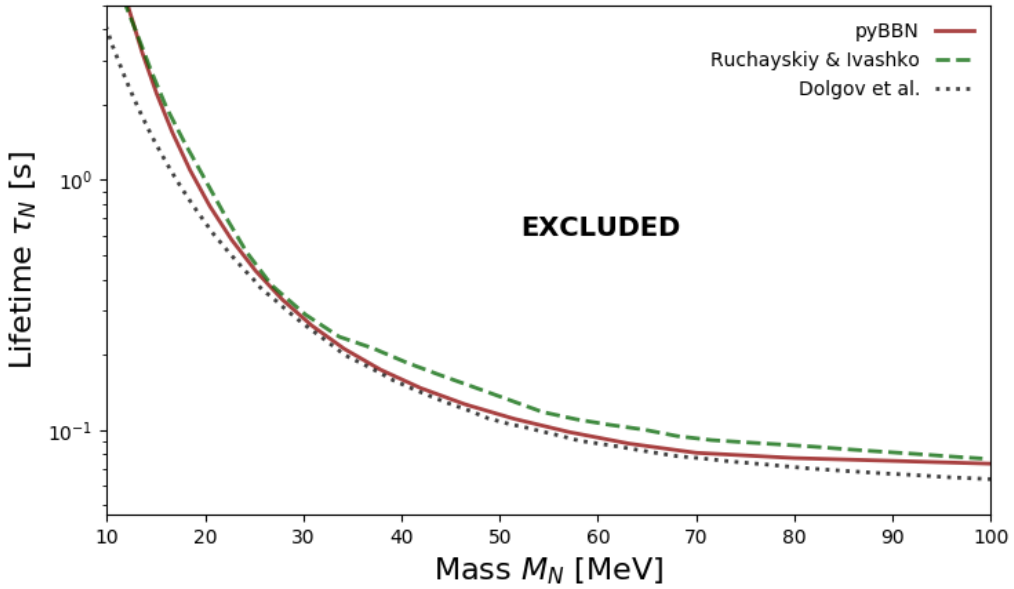

FIGURE 4.3: Bounds on the lifetime of HNLs that mix only with electron neutrino. The ^{4}He abundance in Eq. 4.1 is used to obtain a bound on the mixing angle, which is then converted to a lifetime constraint by Eq. 4.3. Dashed curve is from [25], dotted from [11].

CHAPTER 5

DISCUSSION AND PROSPECTS

The results in Figures 4.1, 4.2 and 4.3 are all consistent with the literature. A number of deviations have been found between the code used in this work and the code of [25], but these do not affect the bounds significantly. All these deviations will be included in the user guide of pyBBN.

The bounds obtained in this work are for HNLs that mix only with electron neutrinos. In general, the mixing pattern can be random. However, it turns out that for masses M_N up to ~ 105 MeV the mixing pattern is not very important, as can be seen in Figures 4, 5 and 6 of [25]. Mixing with muon neutrino only changes the lifetime bound subtly. Once neutrino oscillations are included, the mixing pattern becomes even less important. Therefore, it is the amount of energy injected in the plasma that is more relevant, which depends on the lifetime and mass of the HNL. For higher masses the contribution of HNLs to the expansion rate will probably be an increasingly important factor, since they will dominate the energy density at some point if they have not decayed yet. It is unknown at the moment what holds for masses exceeding 105 MeV, because the decay products themselves will be unstable. For high masses one can therefore expect a shower of decay products, each of which will influence the course of BBN in its own way.

The next step is therefore to apply the machinery discussed in Chapter 3 to HNLs with masses exceeding the muon mass. For masses higher than 1 GeV, the process of hadronization and its inclusion in pyBBN will be the most important procedures to deal with, both of which are as of yet unexplored.

ACKNOWLEDGEMENTS

Many thanks to my supervisors Alexey Boyarsky and Oleg Ruchayskiy for giving me the opportunity to do a research project in this field. I am grateful to Ana Achúcarro for her kindness to be the 2nd corrector of this work. My gratitude also goes to Andrii Magalich, Kyrylo Bondarenko and Shintaro Eijima for their support during this project.

APPENDIX A

Relevant Matrix Elements

The matrix elements listed here are not averaged over any helicities. Subsection A.1 contains the reactions involving SM particles only, Subsection A.2 the reactions involving HNLs above QCD-scale and Subsection A.3 the reactions involving HNLs below QCD-scale. HNL decay channels with a branching ratio of at least 1% for some mass below ~1 GeV are considered in this work (see Figure A.1). The results for HNLs do not take into account charge conjugated channels, which are possible if they are Majorana particles.

The explicit determination of matrix elements involving multiple mesons can be extremely challenging. Therefore, an approximation has been used by assuming the matrix element to be constant and using the definition of decay width,

$$\Gamma = \frac{1}{2gM} \int \left(\prod_i \frac{\mathrm{d}^3 y_i}{(2\pi)^3 2E_i} \right) |\mathscr{M}|^2 (2\pi)^4 \delta^4 (P - \sum_i P_i) \, ,$$

together with its measured value (from e.g. [24]) to solve for $|\mathscr{M}|^2$. For three-particle reactions this method gives the exact matrix element.

The values of the meson decay constants used in Subsection A.3 are from [6] and summarized below.

f_{π^0}	$f_{\pi^\pm}$	f_η	f_{ρ^0}	$f_{\rho^\pm}$	f_ω	$f_{\eta'}$	f_ϕ	
130.2	130.2	81.7	208.9	208.9	195.5	-94.7	229.5	MeV

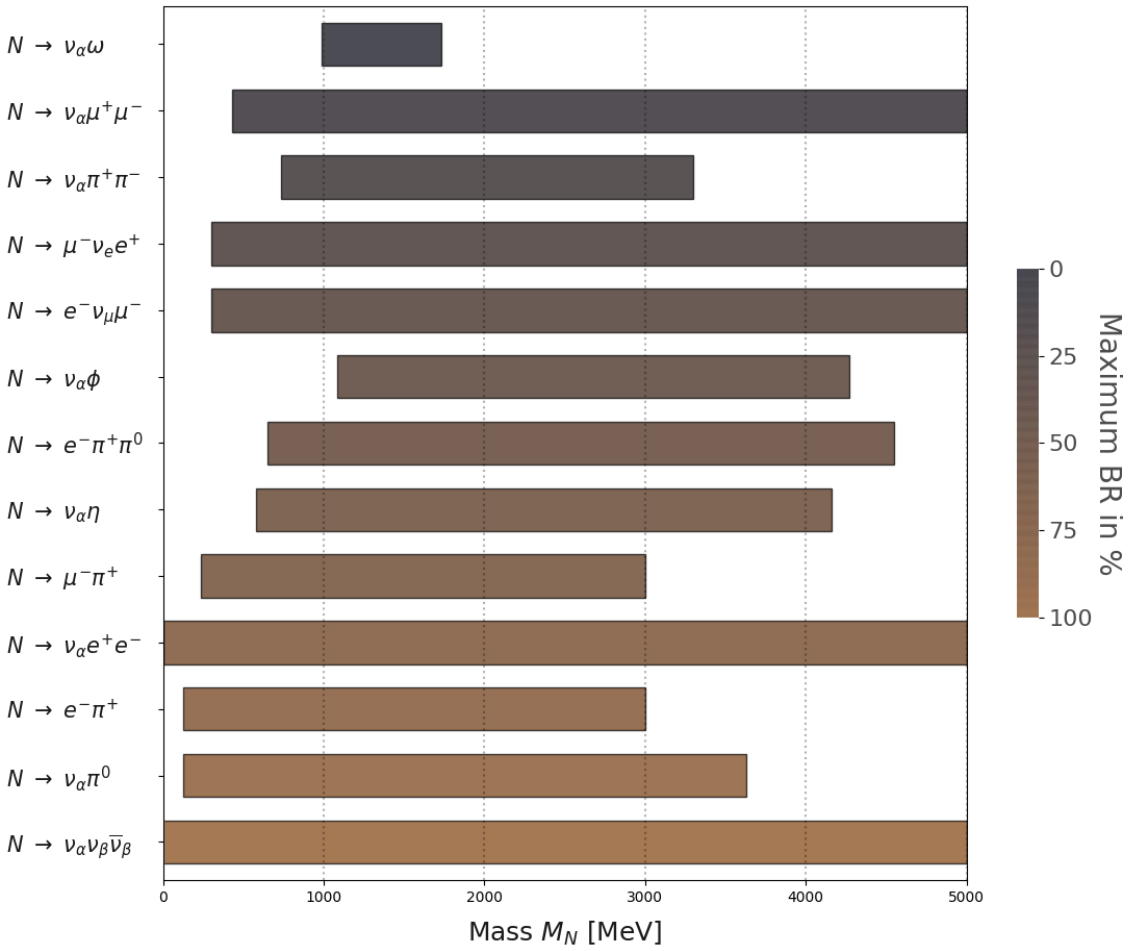

FIGURE A.1: List of HNL decay channels with branching ratios more than 1% for some HNL mass below ~ 1 GeV. The left border indicates the HNL mass where the branching ratio exceeds 1%, the right border when it falls below the 1 % threshold. In this plot a model was assumed where all three mixing angles are equal to each other.

A.1 Matrix elements in the SM

A.1.1 Four-particle processes with leptons

Process $(1+2\to3+4)$	S	$SG_{\mathrm{F}}^2 a^{-4}\lvert\mathscr{M}\rvert^2$
$\nu_\alpha+\nu_\beta\to\nu_\alpha+\nu_\beta$	1	$32(Y_1\cdot Y_2)(Y_3\cdot Y_4)$
$\nu_\alpha+\overline{\nu_\beta}\to\nu_\alpha+\overline{\nu_\beta}$	1	$32(Y_1\cdot Y_4)(Y_2\cdot Y_3)$
$\nu_\alpha+\nu_\alpha\to\nu_\alpha+\nu_\alpha$	$\frac{1}{2}$	$64(Y_1\cdot Y_2)(Y_3\cdot Y_4)$
$\nu_\alpha+\overline{\nu_\alpha}\to\nu_\alpha+\overline{\nu_\alpha}$	1	$128(Y_1\cdot Y_4)(Y_2\cdot Y_3)$
$\nu_\alpha+\overline{\nu_\alpha}\to\nu_\beta+\overline{\nu_\beta}$	1	$32(Y_1\cdot Y_4)(Y_3\cdot Y_2)$
$\nu_e+\overline{\nu_e}\to e^++e^-$	1	$128\Big[g_L^2(Y_1\cdot Y_3)(Y_2\cdot Y_4)+g_R^2(Y_1\cdot Y_4)(Y_2\cdot Y_3)$ $+g_Lg_Ra^2m_e^2(Y_1\cdot Y_2)\Big]$
$\nu_e+e^-\to\nu_e+e^-$	1	$128\Big[g_L^2(Y_1\cdot Y_2)(Y_3\cdot Y_4)+g_R^2(Y_1\cdot Y_4)(Y_3\cdot Y_2)$ $-g_Lg_Ra^2m_e^2(Y_1\cdot Y_3)\Big]$
$\nu_e+e^+\to\nu_e+e^+$	1	$128\Big[g_L^2(Y_1\cdot Y_4)(Y_3\cdot Y_2)+g_R^2(Y_1\cdot Y_2)(Y_3\cdot Y_4)$ $-g_Lg_Ra^2m_e^2(Y_1\cdot Y_3)\Big]$
$\nu_{\mu/\tau}+\overline{\nu_{\mu/\tau}}\to e^++e^-$	1	$128\Big[\widetilde{g_L}^2(Y_1\cdot Y_3)(Y_2\cdot Y_4)+g_R^2(Y_1\cdot Y_4)(Y_2\cdot Y_3)$ $+\widetilde{g_L}g_Ra^2m_e^2(Y_1\cdot Y_2)\Big]$
$\nu_{\mu/\tau}+e^-\to\nu_{\mu/\tau}+e^-$	1	$128\Big[\widetilde{g_L}^2(Y_1\cdot Y_2)(Y_3\cdot Y_4)+g_R^2(Y_1\cdot Y_4)(Y_3\cdot Y_2)$ $-\widetilde{g_L}g_Ra^2m_e^2(Y_1\cdot Y_3)\Big]$
$\nu_{\mu/\tau}+e^+\to\nu_{\mu/\tau}+e^+$	1	$128\Big[\widetilde{g_L}^2(Y_1\cdot Y_4)(Y_3\cdot Y_2)+g_R^2(Y_1\cdot Y_2)(Y_3\cdot Y_4)$ $-\widetilde{g_L}g_Ra^2m_e^2(Y_1\cdot Y_3)\Big]$

TABLE A.1: Squared matrix elements for weak processes involving active neutrinos and electrons/positrons. S is the symmetry factor and $\alpha,\beta\in\{e,\mu,\tau\}$, where $\alpha\neq\beta$. Here: $g_R=\sin^2\theta_{\mathrm{W}}$, $g_L=1/2+\sin^2\theta_{\mathrm{W}}$ and $\widetilde{g_L}=-1/2+\sin^2\theta_{\mathrm{W}}$, with θ_{W} the Weinberg angle.

A.1.2 Three-particle and four-particle meson decays

Process $(1 \to 2+3)$	S	$\lvert\mathscr{M}\rvert^2$
$\pi^0 \to \gamma + \gamma$	1	$\alpha_{\text{em}}^2 m_\pi^4 \left[2\pi^2 f_\pi^2\right]^{-1}$
$\pi^+ \to \mu^+ + \nu_\mu$	1	$2G_{\text{F}}^2 \lvert V_{ud}\rvert^2 f_\pi^2 m_\mu^4 \left[\frac{m_\pi^2}{m_\mu^2} - 1\right]$

TABLE A.2: Squared matrix elements for pion decays.

Process $(1 \to 2+3+4)$	$\lvert\mathscr{M}\rvert^2$
$K^+ \to \pi^0 + e^+ + \nu_e$	$1.42906 \cdot 10^{-13}$
$K^+ \to \pi^+ + \pi^- + \pi^+$	$1.85537 \cdot 10^{-12}$
$K_L^0 \to \pi^\pm + e^\mp + \nu_e$	$2.80345 \cdot 10^{-13}$
$K_L^0 \to \pi^\pm + \mu^\mp + \nu_\mu$	$3.03627 \cdot 10^{-13}$
$K_L^0 \to \pi^0 + \pi^0 + \pi^0$	$1.05573 \cdot 10^{-12}$
$K_L^0 \to \pi^+ + \pi^- + \pi^0$	$8.26989 \cdot 10^{-13}$
$\eta \to \pi^0 + \pi^0 + \pi^0$	$8.70984 \cdot 10^{-2}$
$\eta \to \pi^+ + \pi^- + \pi^0$	$6.90629 \cdot 10^{-2}$
$\eta \to \pi^+ + \pi^- + \gamma$	$4.66530 \cdot 10^{-3}$
$\omega \to \pi^+ + \pi^- + \pi^0$	$1.14569 \cdot 10^{3}$
$\eta' \to \pi^+ + \pi^- + \eta$	$4.38880 \cdot 10^{1}$
$\eta' \to \pi^0 + \pi^0 + \eta$	$2.00986 \cdot 10^{1}$

Process $(1 \to 2+3)$	$\lvert\mathscr{M}\rvert^2$ [MeV^2]
$K^+ \to \pi^+ + \pi^0$	$3.28177 \cdot 10^{-10}$
$K^+ \to \mu^+ + \nu_\mu$	$8.78918 \cdot 10^{-10}$
$K_S^0 \to \pi^+ + \pi^-$	$1.53713 \cdot 10^{-7}$
$K_S^0 \to \pi^0 + \pi^0$	$6.71800 \cdot 10^{-8}$
$\eta \to \gamma + \gamma$	$1.42174 \cdot 10^{1}$
$\rho^0 \to \pi^+ + \pi^-$	$1.86839 \cdot 10^{7}$
$\rho^+ \to \pi^+ + \pi^0$	$1.86390 \cdot 10^{7}$
$\omega \to \pi^0 + \gamma$	$8.55086 \cdot 10^{4}$
$\eta' \to \rho^0 + \gamma$	$8.04463 \cdot 10^{3}$
$\phi \to K^+ + K^-$	$1.28798 \cdot 10^{6}$
$\phi \to K_L^0 + K_S^0$	$1.03471 \cdot 10^{6}$
$\phi \to \rho^0 + \pi^0$	$2.86706 \cdot 10^{5}$

TABLE A.3: Squared matrix elements for meson decays, where the constant matrix element approximation is used. For Majorana particles that can also decay through the charge conjugated channel, the factor of 2 in the decay width is already taken into account here.

A.2 Matrix elements for HNLs above Λ_{QCD}

A.2.1 Four-particle processes with leptons only

Process $(1+2\to3+4)$	S	$SG_{\mathrm{F}}^{-2}a^{-4}\lvert\mathscr{M}\rvert^2$
$N+\nu_\beta\to\nu_\alpha+\nu_\beta$	1	$32\lvert\theta_\alpha\rvert^2(Y_1\cdot Y_2)(Y_3\cdot Y_4)$
$N+\overline{\nu_\beta}\to\nu_\alpha+\overline{\nu_\beta}$	1	$32\lvert\theta_\alpha\rvert^2(Y_1\cdot Y_4)(Y_2\cdot Y_3)$
$N+\nu_\alpha\to\nu_\alpha+\nu_\alpha$	$\frac{1}{2}$	$64\lvert\theta_\alpha\rvert^2(Y_1\cdot Y_2)(Y_3\cdot Y_4)$
$N+\overline{\nu_\alpha}\to\nu_\alpha+\overline{\nu_\alpha}$	1	$128\lvert\theta_\alpha\rvert^2(Y_1\cdot Y_4)(Y_2\cdot Y_3)$
$N+\overline{\nu_\alpha}\to\nu_\beta+\overline{\nu_\beta}$	1	$32\lvert\theta_\alpha\rvert^2(Y_1\cdot Y_4)(Y_3\cdot Y_2)$
$N+\overline{\nu_e}\to e^++e^-$	1	$128\lvert\theta_e\rvert^2\left[g_L^2(Y_1\cdot Y_3)(Y_2\cdot Y_4)+g_R^2(Y_1\cdot Y_4)(Y_2\cdot Y_3)\right.$ $\left.+g_Lg_Ra^2m_e^2(Y_1\cdot Y_2)\right]$
$N+e^-\to\nu_e+e^-$	1	$128\lvert\theta_e\rvert^2\left[g_L^2(Y_1\cdot Y_2)(Y_3\cdot Y_4)+g_R^2(Y_1\cdot Y_4)(Y_3\cdot Y_2)\right.$ $\left.-g_Lg_Ra^2m_e^2(Y_1\cdot Y_3)\right]$
$N+e^+\to\nu_e+e^+$	1	$128\lvert\theta_e\rvert^2\left[g_L^2(Y_1\cdot Y_4)(Y_3\cdot Y_2)+g_R^2(Y_1\cdot Y_2)(Y_3\cdot Y_4)\right.$ $\left.-g_Lg_Ra^2m_e^2(Y_1\cdot Y_3)\right]$
$N+\overline{\nu_{\mu/\tau}}\to e^++e^-$	1	$128\lvert\theta_{\mu/\tau}\rvert^2\left[\widetilde{g_L}^2(Y_1\cdot Y_3)(Y_2\cdot Y_4)+g_R^2(Y_1\cdot Y_4)(Y_2\cdot Y_3)\right.$ $\left.+\widetilde{g_L}g_Ra^2m_e^2(Y_1\cdot Y_2)\right]$
$N+e^-\to\nu_{\mu/\tau}+e^-$	1	$128\lvert\theta_{\mu/\tau}\rvert^2\left[\widetilde{g_L}^2(Y_1\cdot Y_2)(Y_3\cdot Y_4)+g_R^2(Y_1\cdot Y_4)(Y_3\cdot Y_2)\right.$ $\left.-\widetilde{g_L}g_Ra^2m_e^2(Y_1\cdot Y_3)\right]$
$N+e^+\to\nu_{\mu/\tau}+e^+$	1	$128\lvert\theta_{\mu/\tau}\rvert^2\left[\widetilde{g_L}^2(Y_1\cdot Y_4)(Y_3\cdot Y_2)+g_R^2(Y_1\cdot Y_2)(Y_3\cdot Y_4)\right.$ $\left.-\widetilde{g_L}g_Ra^2m_e^2(Y_1\cdot Y_3)\right]$

TABLE A.4: Squared matrix elements for weak processes involving HNLs and leptons. S is the symmetry factor and $\alpha,\beta\in\{e,\mu,\tau\}$, where $\alpha\neq\beta$. Here: $g_R=\sin^2\theta_{\mathrm{W}}$, $g_L=1/2+\sin^2\theta_{\mathrm{W}}$ and $\widetilde{g_L}=-1/2+\sin^2\theta_{\mathrm{W}}$, with θ_{W} the Weinberg angle.

Process $(1+2\to3+4)$	S	$SG_{\mathrm{F}}^{-2}a^{-4}\lvert\mathscr{M}\rvert^2$
$N+\overline{\nu_\mu}\to e^-+\mu^+$	1	$128\lvert\theta_e\rvert^2(Y_1\cdot Y_4)(Y_2\cdot Y_3)$
$N+\overline{\nu_e}\to e^++\mu^-$	1	$128\lvert\theta_\mu\rvert^2(Y_1\cdot Y_3)(Y_2\cdot Y_4)$
$N+e^-\to\nu_e+\mu^-$	1	$128\lvert\theta_\mu\rvert^2(Y_1\cdot Y_2)(Y_3\cdot Y_4)$
$N+e^+\to\nu_\mu+\mu^+$	1	$128\lvert\theta_e\rvert^2(Y_1\cdot Y_4)(Y_3\cdot Y_2)$
$N+\overline{\nu_\mu}\to\mu^++\mu^-$	1	$128\lvert\theta_\mu\rvert^2\left[g_L^2(Y_1\cdot Y_3)(Y_2\cdot Y_4)+g_R^2(Y_1\cdot Y_4)(Y_2\cdot Y_3)\right.$ $\left.+g_Lg_Ra^2m_\mu^2(Y_1\cdot Y_2)\right]$
$N+\overline{\nu_{e/\tau}}\to\mu^++\mu^-$	1	$128\lvert\theta_{e/\tau}\rvert^2\left[\widetilde{g_L}^2(Y_1\cdot Y_3)(Y_2\cdot Y_4)+g_R^2(Y_1\cdot Y_4)(Y_2\cdot Y_3)\right.$ $\left.+\widetilde{g_L}g_Ra^2m_\mu^2(Y_1\cdot Y_2)\right]$

Process $(1\to2+3+4)$	S	$SG_{\mathrm{F}}^{-2}a^{-4}\lvert\mathscr{M}\rvert^2$
$N\to\nu_\alpha+\nu_\beta+\overline{\nu_\beta}$	1	$32\lvert\theta_\alpha\rvert^2(Y_1\cdot Y_4)(Y_2\cdot Y_3)$
$N\to\nu_\alpha+\nu_\alpha+\overline{\nu_\alpha}$	$\frac{1}{2}$	$64\lvert\theta_\alpha\rvert^2(Y_1\cdot Y_4)(Y_2\cdot Y_3)$
$N\to\nu_e+e^++e^-$	1	$128\lvert\theta_e\rvert^2\left[g_L^2(Y_1\cdot Y_3)(Y_2\cdot Y_4)+g_R^2(Y_1\cdot Y_4)(Y_2\cdot Y_3)\right.$ $\left.+g_Lg_Ra^2m_e^2(Y_1\cdot Y_2)\right]$
$N\to\nu_{\mu/\tau}+e^++e^-$	1	$128\lvert\theta_{\mu/\tau}\rvert^2\left[\widetilde{g_L}^2(Y_1\cdot Y_3)(Y_2\cdot Y_4)+g_R^2(Y_1\cdot Y_4)(Y_2\cdot Y_3)\right.$ $\left.+\widetilde{g_L}g_Ra^2m_e^2(Y_1\cdot Y_2)\right]$
$N\to\nu_\mu+e^-+\mu^+$	1	$128\lvert\theta_e\rvert^2(Y_1\cdot Y_4)(Y_2\cdot Y_3)$
$N\to\nu_e+e^++\mu^-$	1	$128\lvert\theta_\mu\rvert^2(Y_1\cdot Y_3)(Y_2\cdot Y_4)$
$N\to\nu_\mu+\mu^++\mu^-$	1	$128\lvert\theta_\mu\rvert^2\left[g_L^2(Y_1\cdot Y_3)(Y_2\cdot Y_4)+g_R^2(Y_1\cdot Y_4)(Y_2\cdot Y_3)\right.$ $\left.+g_Lg_Ra^2m_\mu^2(Y_1\cdot Y_2)\right]$
$N\to\nu_{e/\tau}+\mu^++\mu^-$	1	$128\lvert\theta_{e/\tau}\rvert^2\left[\widetilde{g_L}^2(Y_1\cdot Y_3)(Y_2\cdot Y_4)+g_R^2(Y_1\cdot Y_4)(Y_2\cdot Y_3)\right.$ $\left.+\widetilde{g_L}g_Ra^2m_\mu^2(Y_1\cdot Y_2)\right]$

TABLE A.5: Squared matrix elements for weak processes involving HNLs and leptons. Note: low temperatures are assumed here. At high temperatures, reactions such as $N+\mu^-\to e^-+\nu_\mu$ are possible. The corresponding matrix elements can be trivially deduced from the ones given above.

A.2.2 Four-particle processes with leptons and quarks

Process $(1+2\to3+4)$	S	$SG_{\mathrm{F}}^{-2}a^{-4}\lvert\mathscr{M}\rvert^2$
$N+\ell_\alpha^+\to U+\overline{D}$	1	$128\lvert\theta_\alpha\rvert^2\lvert V_{ud}\rvert^2(Y_1\cdot Y_4)(Y_2\cdot Y_3)$
$N+D\to\ell_\alpha^-+U$	1	$128\lvert\theta_\alpha\rvert^2\lvert V_{ud}\rvert^2(Y_1\cdot Y_2)(Y_3\cdot Y_4)$
$N+\overline{U}\to\ell_\alpha^-+\overline{D}$	1	$128\lvert\theta_\alpha\rvert^2\lvert V_{ud}\rvert^2(Y_1\cdot Y_4)(Y_3\cdot Y_2)$
$N+\overline{\nu_\alpha}\to\overline{U}+U$	1	$\frac{32}{9}\lvert\theta_\alpha\rvert^2\Big[16g_R^2(Y_1\cdot Y_4)(Y_2\cdot Y_3)$ $+(3-4g_R)^2(Y_1\cdot Y_3)(Y_2\cdot Y_4)$ $+4g_R\theta_W(4g_R-3)a^2m_U^2(Y_1\cdot Y_2)\Big]$
$N+U\to\nu_\alpha+U$	1	$\frac{32}{9}\lvert\theta_\alpha\rvert^2\Big[16g_R^2(Y_1\cdot Y_4)(Y_2\cdot Y_3)$ $+(3-4g_R)^2(Y_1\cdot Y_2)(Y_3\cdot Y_4)$ $-4g_R(4g_R-3)a^2m_U^2(Y_1\cdot Y_3)\Big]$
$N+\overline{U}\to\nu_\alpha+\overline{U}$	1	$\frac{32}{9}\lvert\theta_\alpha\rvert^2\Big[16g_R^2(Y_1\cdot Y_2)(Y_3\cdot Y_4)$ $+(3-4g_R)^2(Y_1\cdot Y_4)(Y_3\cdot Y_2)$ $-4g_R(4g_R-3)a^2m_U^2(Y_1\cdot Y_3)\Big]$
$N+\overline{\nu_\alpha}\to\overline{D}+D$	1	$\frac{32}{9}\lvert\theta_\alpha\rvert^2\Big[4g_R^2(Y_1\cdot Y_4)(Y_2\cdot Y_3)$ $+(3-2g_R)^2(Y_1\cdot Y_3)(Y_2\cdot Y_4)$ $+2g_R(2g_R-3)a^2m_D^2(Y_1\cdot Y_2)\Big]$
$N+D\to\nu_\alpha+D$	1	$\frac{32}{9}\lvert\theta_\alpha\rvert^2\Big[4g_R^2(Y_1\cdot Y_4)(Y_2\cdot Y_3)$ $+(3-2g_R)^2(Y_1\cdot Y_2)(Y_3\cdot Y_4)$ $-2g_R(2g_R-3)a^2m_D^2(Y_1\cdot Y_3)\Big]$
$N+\overline{D}\to\nu_\alpha+\overline{D}$	1	$\frac{32}{9}\lvert\theta_\alpha\rvert^2\Big[4g_R^2(Y_1\cdot Y_2)(Y_3\cdot Y_4)$ $+(3-2g_R)^2(Y_1\cdot Y_4)(Y_3\cdot Y_2)$ $-2g_R(2g_R-3)a^2m_D^2(Y_1\cdot Y_3)\Big]$

TABLE A.6: Squared matrix elements for weak processes involving HNLs, leptons and quarks. Here: U are up-type quarks, D down-type quarks and $g_R=\sin^2\theta_{\mathrm{W}}$.

Process $(1 \to 2+3+4)$	S	$SG_{\mathrm{F}}^{-2}a^{-4}\lvert\mathscr{M}\rvert^2$
$N \to \ell_\alpha^- + U + \overline{D}$	1	$128\lvert\theta_\alpha\rvert^2\lvert V_{ud}\rvert^2(Y_1\cdot Y_4)(Y_2\cdot Y_3)$
$N \to \nu_\alpha + \overline{U} + U$	1	$\frac{32}{9}\lvert\theta_\alpha\rvert^2\Big[16g_R^2(Y_1\cdot Y_4)(Y_2\cdot Y_3)$ $+(3-4g_R)^2(Y_1\cdot Y_3)(Y_2\cdot Y_4)$ $+4g_R(4g_R-3)a^2m_U^2(Y_1\cdot Y_2)\Big]$
$N \to \nu_\alpha + \overline{D} + D$	1	$\frac{32}{9}\lvert\theta_\alpha\rvert^2\Big[4g_R^2(Y_1\cdot Y_4)(Y_2\cdot Y_3)$ $+(3-2g_R)^2(Y_1\cdot Y_3)(Y_2\cdot Y_4)$ $+2g_R(2g_R-3)a^2m_D^2(Y_1\cdot Y_2)\Big]$

A.3 Matrix elements for HNLs below Λ_{QCD}

In addition to interactions with leptons, HNLs will also decay into mesons.

A.3.1 Three-particle processes with single mesons

Process $(1 \to 2+3$ or $1+2 \to 3)$	S	$SG_{\mathrm{F}}^{-2}M_N^{-4}\lvert\mathscr{M}\rvert^2$
$N \to \nu_\alpha + \pi^0$	1	$\lvert\theta_\alpha\rvert^2 f_\pi^2\left[1-\frac{m_\pi^2}{M_N^2}\right]$
$N \to \ell_\alpha^\mp + \pi^\pm$	1	$2\lvert\theta_\alpha\rvert^2\lvert V_{ud}\rvert^2 f_\pi^2\left[\left(1-\frac{m_{\ell_\alpha}^2}{M_N^2}\right)^2-\frac{m_\pi^2}{M_N^2}\left(1+\frac{m_{\ell_\alpha}^2}{M_N^2}\right)\right]$
$N \to \nu_\alpha + \eta$	1	$\lvert\theta_\alpha\rvert^2 f_\eta^2\left[1-\frac{m_\eta^2}{M_N^2}\right]$
$N \to \nu_\alpha + \rho^0$	1	$\lvert\theta_\alpha\rvert^2\left(1-2\sin^2\theta_{\mathrm{W}}\right)^2 f_\rho^2\left[1+2\frac{m_\rho^2}{M_N^2}\right]\left[1-\frac{m_\rho^2}{M_N^2}\right]$
$N \to \ell_\alpha^\mp + \rho^\pm$	1	$2\lvert\theta_\alpha\rvert^2\lvert V_{ud}\rvert^2 f_\rho^2\left[\left(1-\frac{m_{\ell_\alpha}^2}{M_N^2}\right)^2+\frac{m_\rho^2}{M_N^2}\left(1+\frac{m_{\ell_\alpha}^2}{M_N^2}\right)\right.$ $\left.-2\frac{m_\rho^4}{M_N^4}\right]$
$N \to \nu_\alpha + \omega$	1	$\lvert\theta_\alpha\rvert^2\left(\frac{4}{3}\sin^2\theta_{\mathrm{W}}\right)^2 f_\omega^2\left[1+2\frac{m_\omega^2}{M_N^2}\right]\left[1-\frac{m_\omega^2}{M_N^2}\right]$
$N \to \nu_\alpha + \eta'$	1	$\lvert\theta_\alpha\rvert^2 f_{\eta'}^2\left[1-\frac{m_{\eta'}^2}{M_N^2}\right]$
$N \to \nu_\alpha + \phi$	1	$\lvert\theta_\alpha\rvert^2\left(\frac{4}{3}\sin^2\theta_{\mathrm{W}}-1\right)^2 f_\phi^2\left[1+2\frac{m_\phi^2}{M_N^2}\right]\left[1-\frac{m_\phi^2}{M_N^2}\right]$

TABLE A.7: Squared matrix elements for HNL decays into mesons.

APPENDIX B

COLLISION INTEGRALS

Consider the Boltzmann equation in comoving coordinates:

$$\frac{\mathrm{d}f_1}{\mathrm{d}t} = \frac{\mathrm{d}f_1}{\mathrm{d}\ln a}\frac{\mathrm{d}\ln a}{\mathrm{d}t} = \frac{\mathrm{d}f_1}{\mathrm{d}\ln a}H = \sum_{\text{reactions}} I_{\text{coll}} \,, \tag{B.1}$$

with

$$I_{\text{coll}} = \frac{a^{7-2Q}}{2g\widetilde{E_1}} \sum_{\text{in,out}} \int \left(\prod_{i=2}^{Q} \frac{\mathrm{d}^3 y_i}{(2\pi)^3 2\widetilde{E_i}} \right) S|\mathscr{M}|^2 F[f] (2\pi)^4 \delta^4(Y_{\text{in}} - Y_{\text{out}}) \tag{B.2}$$

The delta function can be rewritten as

$$\delta^4(Y_{\text{in}} - Y_{\text{out}}) = \delta^4(s_1 Y_1 + s_2 Y_2 + ... + s_Q Y_Q) \,, \tag{B.3}$$

with $s_i = \{-1, 1\}$ if particle i is on the {left, right}-hand side of the reaction. The $Y_i = aP_i$ here are the comoving four-momenta.

B.1 Three-particle collision integral

$$I_{\text{coll}} = \frac{a}{2\widetilde{E_1}} \int \frac{\mathrm{d}^3 y_2 \mathrm{d}^3 y_3}{(2g\pi)^6 2\widetilde{E_2} 2\widetilde{E_3}} S|\mathscr{M}|^2 F[f] (2\pi)^4 \delta^4(s_1 Y_1 + s_2 Y_2 + s_3 Y_3) \tag{B.4}$$

B.1.1 Case $y_1 \neq 0$

Since a homogeneous and isotropic universe is assumed, only absolute values of momenta are relevant. Moreover, the matrix element in three particle interactions is independent of the four-momenta.

$$I_{\text{coll}} = \frac{S|\mathscr{M}|^2 a}{8(2\pi)^2 g\widetilde{E_1}} \int \frac{\mathrm{d}y_2 \mathrm{d}y_3 \mathrm{d}\Omega_2 \mathrm{d}\Omega_3 y_2^2 y_3^2}{\widetilde{E_2}\widetilde{E_3}} F[f]\delta^4(s_1 Y_1 + s_2 Y_2 + s_3 Y_3) \tag{B.5}$$

Using the identity

$$\delta^3(s_1\mathbf{y_1} + s_2\mathbf{y_2} + s_3\mathbf{y_3}) = \frac{1}{(2\pi)^3} \int \mathrm{d}\lambda \mathrm{d}\Omega_\lambda \lambda^2 e^{i(s_1\mathbf{y_1} + s_2\mathbf{y_2} + s_3\mathbf{y_3})\cdot\boldsymbol{\lambda}} \tag{B.6}$$

gives

$$\begin{aligned}
I_{\text{coll}} =& \frac{S|\mathscr{M}|^2 a}{8(2\pi)^5 g\widetilde{E_1}} \int \frac{\mathrm{d}y_2 \mathrm{d}y_3 y_2^2 y_3^2}{\widetilde{E_2}\widetilde{E_3}} F[f]\delta(s_1\widetilde{E_1} + s_2\widetilde{E_2} + s_3\widetilde{E_3}) \cdot \\
& \cdot \int \mathrm{d}\lambda \lambda^2 \int \mathrm{d}\Omega_\lambda e^{i s_1 y_1 \lambda \cos\theta_\lambda} \int \mathrm{d}\Omega_2 e^{i s_1 y_2 \lambda \cos\theta_2} \int \mathrm{d}\Omega_3 e^{i s_1 y_3 \lambda \cos\theta_3} \\
=& \frac{S|\mathscr{M}|^2 a}{8(2\pi)^5 g\widetilde{E_1}} \int \frac{\mathrm{d}y_2 \mathrm{d}y_3 y_2^2 y_3^2}{\widetilde{E_2}\widetilde{E_3}} F[f]\delta(s_1\widetilde{E_1} + s_2\widetilde{E_2} + s_3\widetilde{E_3}) \cdot \\
& \cdot \int \mathrm{d}\lambda \lambda^2 \left(4\pi \frac{\sin(y_1\lambda)}{y_1\lambda}\right)\left(4\pi \frac{\sin(y_2\lambda)}{y_2\lambda}\right)\left(4\pi \frac{\sin(y_3\lambda)}{y_3\lambda}\right) \\
=& \frac{S|\mathscr{M}|^2 a}{(2\pi)^2 g\widetilde{E_1} y_1} \int \frac{\mathrm{d}y_2 \mathrm{d}y_3 y_2 y_3}{\widetilde{E_2}\widetilde{E_3}} F[f]\delta(s_1\widetilde{E_1} + s_2\widetilde{E_2} + s_3\widetilde{E_3}) \cdot \\
& \cdot \int \frac{\mathrm{d}\lambda}{\lambda} \sin(y_1\lambda)\sin(y_2\lambda)\sin(y_3\lambda)
\end{aligned} \tag{B.7}$$

Rewrite the delta function of energies as

$$\begin{aligned}
\int \frac{\mathrm{d}y_3 y_3}{\widetilde{E_3}} \delta(s_1\widetilde{E_1} + s_2\widetilde{E_2} + s_3\widetilde{E_3}) &= \int \mathrm{d}y_3 \frac{y_3}{\widetilde{E_3}} \frac{\delta\left(y_3 - y_3^*\right)}{\frac{y_3^*}{\widetilde{E_3^*}}} \theta\left((s_1\widetilde{E_1} + s_2\widetilde{E_2})^2 - a^2 m_3^2\right) \\
&= \int \mathrm{d}y_3 \frac{y_3}{\widetilde{E_3}} \frac{\widetilde{E_3^*}}{y_3^*} \delta(y_3 - y_3^*)\, \theta\left(\left(\widetilde{E_3^*}\right)^2 - a^2 m_3^2\right) ,
\end{aligned} \tag{B.8}$$

where $\left(\widetilde{E_3^*}\right)^2 = \left(y_3^*\right)^2 + \frac{x^2}{M^2} m_3^2 = \left(s_1\widetilde{E_1} + s_2\widetilde{E_2}\right)^2$ and $y_3^* = \sqrt{(s_1\widetilde{E_1} + s_2\widetilde{E_2})^2 - a^2 m_3^2}$.

Plugging Eq. (B.8) in Eq. (B.7) above:

$$I_{\text{coll}} = \frac{S|\mathscr{M}|^2 a}{(2\pi)^2 g \widetilde{E_1} y_1} \int \frac{\mathrm{d}y_2 y_2}{\widetilde{E_2}} F[f] \int \frac{\mathrm{d}\lambda}{\lambda} \sin(y_1\lambda)\sin(y_2\lambda)\sin(y_3^*\lambda)\theta\left(\left(\widetilde{E_3^*}\right)^2 - a^2 m_3^2\right)$$

Now, the integral over λ is equal to

$$\mathscr{X} = \frac{\pi}{8}\left(-\text{Sgn}[y_1 - y_2 - y_3^*] + \text{Sgn}[y_1 + y_2 - y_3^*] + \text{Sgn}[y_1 - y_2 + y_3^*] - 1\right) , \tag{B.9}$$

with Sgn the signum function and where $y_1 \geq y_2 \geq y_3$ is assumed.
The final form is then

$$I_{\text{coll}} = \frac{S|\mathscr{M}|^2 a}{(2\pi)^2 g \widetilde{E_1} y_1} \int \frac{\mathrm{d}y_2 y_2}{\widetilde{E_2}} \mathscr{X}\theta\left(\left(s_1\widetilde{E_1} + s_2\widetilde{E_2}\right)^2 - a^2 m_3^2\right)(F[f])\Big|_{y_3 = y_3^*} \tag{B.10}$$

B.1.2 Case $y_1 = 0$

$$\begin{aligned}
I_{\text{coll}} &= \frac{S|\mathscr{M}|^2 a}{8(2\pi)^2 g a m_1} \int \frac{\mathrm{d}^3 y_2 \mathrm{d}^3 y_3}{\widetilde{E_2}\widetilde{E_3}} F[f]\delta\left(s_1 a m_1 + s_2\widetilde{E_2} + s_3\widetilde{E_3}\right)\delta^3(s_2\mathbf{y_2} + s_3\mathbf{y_3}) \\
&= \frac{S|\mathscr{M}|^2}{8(2\pi)^2 g m_1} \int \mathrm{d}^3 y_2 F[f]\delta\left(s_1 a m_1 + s_2\sqrt{y_2^2 + (am_2)^2} + s_3\sqrt{y_2^2 + (am_3)^2}\right) \cdot \\
&\quad \cdot \left(\sqrt{y_2^2 + (am_2)^2}\sqrt{y_2^2 + (am_3)^2}\right)^{-1} \\
&= \frac{S|\mathscr{M}|^2}{8\pi g m_1} \int \mathrm{d}y_2 y_2^2 F[f]\delta\left(y_2 - y_2^*\right)\left|\frac{s_2 y_2^*}{\sqrt{(y_2^*)^2 + a^2 m_2^2}} + \frac{s_3 y_2^*}{\sqrt{(y_2^*)^2 + a^2 m_3^2}}\right|^{-1} \cdot \\
&\quad \cdot \left(\sqrt{y_2^2 + (am_2)^2}\sqrt{y_2^2 + (am_3)^2}\right)^{-1} \theta\left(\left(s_1 a m_1 + s_2\widetilde{E_2}\right)^2 - a^2 m_3^2\right) \\
&= \frac{S|\mathscr{M}|^2}{8\pi g m_1} y_2^* \left|s_2\sqrt{\left(y_2^*\right)^2 + (am_3)^2} + s_3\sqrt{\left(y_2^*\right)^2 + (am_2)^2}\right|^{-1} \theta\left(\left(\widetilde{E_3^*}\right)^2 - a^2 m_3^2\right) \cdot \\
&\quad \cdot (F[f])\Big|_{y_1=0,\ y_2=y_2^*,\ y_3=-y_2^*} \\
&= \frac{S|\mathscr{M}|^2}{8\pi g m_1} y_2^* |s_1 s_2 s_3 a m_1|^{-1} \theta\left(\left(\widetilde{E_3^*}\right)^2 - a^2 m_3^2\right)(F[f])\Big|_{y_1=0,\ y_2=y_2^*,\ y_3=-y_2^*} \\
&= \frac{S|\mathscr{M}|^2}{8\pi g m_1^2} \frac{y_2^*}{a} \theta\left(\left(\widetilde{E_3^*}\right)^2 - a^2 m_3^2\right)(F[f])\Big|_{y_1=0,\ y_2=y_2^*,\ y_3=-y_2^*} ,
\end{aligned} \tag{B.11}$$

with $\left(\widetilde{E_3^*}\right)^2 = \left(s_1 a m_1 + s_2\widetilde{E_2}\right)^2$ and $y_2^* = a\sqrt{\frac{\left(m_1^2 - m_2^2 - m_3^2\right)^2 - 4m_2^2 m_3^2}{4m_1^2}}$.

B.2 Four-particle collision integral

$$I_{\text{coll}} = \frac{1}{2g\widetilde{E_1}}\frac{1}{a}\int \frac{\mathrm{d}^3y_2\mathrm{d}^3y_3\mathrm{d}y_4^3}{(2\pi)^9 8\widetilde{E_2}\widetilde{E_3}\widetilde{E_4}} S|\mathscr{M}|^2 F[f](2\pi)^4\delta^4(s_1Y_1+s_2Y_2+s_3Y_3+s_4Y_4) \tag{B.12}$$

As can be seen in Appendix A, $|\mathscr{M}|^2$ can be written as

$$|\mathscr{M}|^2 = \frac{1}{a^4}\sum_{i\neq j\neq k\neq l}\left[K_1(Y_i\cdot Y_j)(Y_k\cdot Y_l)+K_2a^2m_im_j(Y_k\cdot Y_l)\right] \tag{B.13}$$

A similar procedure as with the three-particle case is followed here.

B.2.1 Case $y_1 \neq 0$

$$\begin{aligned}
I_{\text{coll}} =& \frac{S}{16(2\pi)^5 g\widetilde{E_1}a}\int\frac{\mathrm{d}y_2\mathrm{d}y_3\mathrm{d}y_4y_2^2y_3^2y_4^2}{\widetilde{E_2}\widetilde{E_3}\widetilde{E_4}}F[f]\delta\left(s_1\widetilde{E_1}+s_2\widetilde{E_2}+s_3\widetilde{E_3}+s_4\widetilde{E_4}\right)\cdot\\
&\cdot\int\mathrm{d}\Omega_2\mathrm{d}\Omega_3\mathrm{d}\Omega_4|\mathscr{M}|^2|\delta^3(s_1\mathbf{y_1}+s_2\mathbf{y_2}+s_3\mathbf{y_3}+s_4\mathbf{y_4})\\
=&\frac{S}{64\pi^3 g\widetilde{E_1}y_1a^5}\int\frac{\mathrm{d}y_2\mathrm{d}y_3\mathrm{d}y_4y_2y_3y_4}{\widetilde{E_2}\widetilde{E_3}\widetilde{E_4}}F[f]\delta\left(s_1\widetilde{E_1}+s_2\widetilde{E_2}+s_3\widetilde{E_3}s_4\widetilde{E_4}\right)\cdot\\
&\cdot\mathscr{D}(Y_1,Y_2,Y_3,Y_4)\,,
\end{aligned} \tag{B.14}$$

with

$$\begin{aligned}
\mathscr{D}(Y_1,Y_2,Y_3,Y_4) =& \frac{y_1y_2y_3y_4}{64\pi^5}\int\mathrm{d}\Omega_2\mathrm{d}\Omega_3\mathrm{d}\Omega_4|\mathscr{M}|^2|\delta^3(s_1\mathbf{y_1}+s_2\mathbf{y_2}+s_3\mathbf{y_3}+s_4\mathbf{y_4})\\
=&\frac{y_1y_2y_3y_4}{64\pi^5}\int\mathrm{d}\lambda\lambda^2\int\mathrm{d}\Omega_\lambda e^{is_1\mathbf{y_1}\cdot\boldsymbol{\lambda}}\int\mathrm{d}\Omega_2e^{is_2\mathbf{y_2}\cdot\boldsymbol{\lambda}}\int\mathrm{d}\Omega_3e^{is_3\mathbf{y_3}\cdot\boldsymbol{\lambda}}\cdot\\
&\cdot\int\mathrm{d}\Omega_4e^{is_4\mathbf{y_4}\cdot\boldsymbol{\lambda}}\sum_{i\neq j\neq k\neq l}\left[K_1(Y_i\cdot Y_j)(Y_k\cdot Y_l)+K_2a^2m_im_j(Y_k\cdot Y_l)\right]\\
=&\frac{y_1y_2y_3y_4}{64\pi^5}\sum_{i\neq j\neq k\neq l}\int\mathrm{d}\lambda\lambda^2\int\mathrm{d}\Omega_\lambda e^{is_iy_i\lambda\cos\theta_i}\int\mathrm{d}\Omega_je^{is_jy_j\lambda\cos\theta_j}\cdot\\
&\cdot\int\mathrm{d}\Omega_ke^{is_ky_k\lambda\cos\theta_k}\int\mathrm{d}\Omega_le^{is_ly_l\lambda\cos\theta_l}\left[K_1(Y_i\cdot Y_j)(Y_k\cdot Y_l)+\right.\\
&\left.+K_2a^2m_im_j(Y_k\cdot Y_l)\right]
\end{aligned} \tag{B.15}$$

Working out the inner products

$$\begin{aligned}
Y_i\cdot Y_j =& \widetilde{E_i}\widetilde{E_j}-\mathbf{y_i}\cdot\mathbf{y_j}=\widetilde{E_i}\widetilde{E_j}-y_iy_j\cos\theta_{ij}\\
=&\widetilde{E_i}\widetilde{E_j}-y_iy_j\left(\cos\theta_i\cos\theta_j+\cos(\phi_i-\phi_j)\sin\theta_i\sin\theta_j\right)\,,
\end{aligned} \tag{B.16}$$

where θ_{ij} is the angle between vectors $\mathbf{y_i}$ and $\mathbf{y_j}$, and using that

$$\int_0^\pi \int_0^{2\pi} \mathrm{d}\theta_i \mathrm{d}\phi_i e^{is_i y_i \lambda \cos\theta_i} \sin^2\theta_i \cos(\phi_i - \phi_j) = 0 \tag{B.17}$$

gives

$$\begin{aligned}\mathscr{D}(Y_1,Y_2,Y_3,Y_4) = &\frac{y_1 y_2 y_3 y_4}{64\pi^5} \sum_{i\neq j\neq k\neq l} \int \mathrm{d}\lambda \lambda^2 \int \mathrm{d}\theta_i \mathrm{d}\phi_i \sin\theta_i e^{is_i y_i \lambda \cos\theta_i} \cdot \\ &\cdot \int \mathrm{d}\theta_j \mathrm{d}\phi_j \sin\theta_j e^{is_j y_j \lambda \cos\theta_j} \int \mathrm{d}\theta_k \mathrm{d}\phi_k \sin\theta_k e^{is_k y_k \lambda \cos\theta_k} \cdot \\ &\cdot \int \mathrm{d}\theta_l \mathrm{d}\phi_l \sin\theta_l e^{is_l y_l \lambda \cos\theta_l} \left[K_1 \left(\widetilde{E_i}\widetilde{E_j} - y_i y_j \cos\theta_i \cos\theta_j\right) \cdot \right. \\ &\left. \cdot \left(\widetilde{E_k}\widetilde{E_l} - y_k y_l \cos\theta_k \cos\theta_l\right) + K_2 a^2 m_i m_j \left(\widetilde{E_k}\widetilde{E_l} - y_k y_l \cos\theta_k \cos\theta_l\right)\right]\end{aligned} \tag{B.18}$$

The integrals over the angles are given by

$$\int_0^\pi \int_0^{2\pi} \mathrm{d}\theta \mathrm{d}\phi \sin\theta e^{isy\lambda\cos\theta} = 4\pi \frac{\sin(y\lambda)}{y\lambda} \tag{B.19}$$

$$\int_0^\pi \int_0^{2\pi} \mathrm{d}\theta \mathrm{d}\phi \sin\theta \cos\theta e^{isy\lambda\cos\theta} = \frac{4\pi}{isy\lambda}\left[\cos(y\lambda) - \frac{\sin(y\lambda)}{y\lambda}\right] \tag{B.20}$$

$$\tag{B.21}$$

and working out all the brackets gives

$$\begin{aligned}\mathscr{D}(Y_1,Y_2,Y_3,Y_4) = \sum_{i\neq j\neq k\neq l} &\left[K_1 \left\{\widetilde{E_1}\widetilde{E_2}\widetilde{E_3}\widetilde{E_4} D_1(y_1,y_2,y_3,y_4) + \widetilde{E_i}\widetilde{E_j} D_2\left(y_i,y_j,y_k,y_l\right) + \right.\right. \\ &+ \left.\widetilde{E_k}\widetilde{E_l} D_2\left(y_k,y_l,y_i,y_j\right) + D_3(y_1,y_2,y_3,y_4)\right\} + \\ &\left.+ K_2 a^2 m_i m_j \left\{\widetilde{E_k}\widetilde{E_l} D_1(y_1,y_2,y_3,y_4) + D_2\left(y_i,y_j,y_k,y_l\right)\right\}\right],\end{aligned} \tag{B.22}$$

with

$$D_1\left(y_i,y_j,y_k,y_l\right) = \frac{4}{\pi}\int \frac{\mathrm{d}\lambda}{\lambda^2} \sin(y_i\lambda)\sin(y_j\lambda)\sin(y_k\lambda)\sin(y_l\lambda) \tag{B.23}$$

$$\begin{aligned}D_2\left(y_i,y_j,y_k,y_l\right) = &s_k s_l \frac{4y_k y_l}{\pi} \int \frac{\mathrm{d}\lambda}{\lambda^2} \sin(y_i\lambda)\sin(y_j\lambda)\left[\cos(y_k\lambda) - \frac{\sin(y_k\lambda)}{y_k\lambda}\right] \cdot \\ &\cdot \left[\cos(y_l\lambda) - \frac{\sin(y_l\lambda)}{y_l\lambda}\right]\end{aligned} \tag{B.24}$$

$$\begin{aligned}D_3\left(y_i,y_j,y_k,y_l\right) = &s_i s_j s_k s_l \frac{4y_i y_j y_k y_l}{\pi} \int \frac{\mathrm{d}\lambda}{\lambda^2} \left[\cos(y_i\lambda) - \frac{\sin(y_i\lambda)}{y_i\lambda}\right]\left[\cos(y_j\lambda) - \frac{\sin(y_j\lambda)}{y_j\lambda}\right] \cdot \\ &\cdot \left[\cos(y_k\lambda) - \frac{\sin(y_k\lambda)}{y_k\lambda}\right]\left[\cos(y_l\lambda) - \frac{\sin(y_l\lambda)}{y_l\lambda}\right]\end{aligned} \tag{B.25}$$

All these three functions are symmetric under the exchange $y_i \leftrightarrow y_j$ and $y_k \leftrightarrow y_l$, which then allows to take $y_i > y_j$ and $y_k > y_l$. Integrating out λ gives the functions in terms of polynomials for all possible cases (factors $s_k s_l$ and $s_i s_j s_k s_l$ omitted):

- $y_i > y_j + y_k + y_l$ or $y_k > y_i + y_j + y_l$:

$$D_1 = D_2 = D_3 = 0$$

- $y_i + y_j > y_k + y_l$ and $y_i + y_l < y_j + y_k$:

$$\begin{aligned} D_1 &= y_l \\ D_2 &= \frac{1}{3} y_l^3 \\ D_3 &= \frac{1}{30} y_l^3 \left[5\left(y_i^2 + y_j^2 + y_k^2\right) - y_l^2 \right] \end{aligned}$$

- $y_i + y_j > y_k + y_l$ and $y_i + y_l > y_j + y_k$:

$$\begin{aligned} D_1 &= \frac{1}{2}(y_j + y_k + y_l - y_i) \\ D_2 &= \frac{1}{12}\left[(y_i - y_j)\left\{ (y_i - y_j)^2 - 3\left(y_k^2 + y_l^2\right) \right\} + 2\left(y_k^3 + y_l^3\right) \right] \\ D_3 &= \frac{1}{60}\left[y_i^5 - y_j^5 - y_k^5 - y_l^5 + 5\left(-y_i^3 y_j^2 + y_i^2 y_j^3 - y_i^3 y_k^2 + y_i^2 y_k^3 \right.\right. \\ &\qquad \left.\left. - y_i^3 y_l^2 + y_i^2 y_l^3 + y_j^3 y_k^2 + y_j^2 y_k^3 + y_j^3 y_l^2 + y_j^2 y_l^3 + y_k^3 y_l^2 + y_k^2 y_l^3 \right) \right] \end{aligned}$$

- $y_i + y_j < y_k + y_l$ and $y_i + y_l > y_j + y_k$:

$$\begin{aligned} D_1 &= y_j \\ D_2 &= \frac{1}{6} y_j \left[3\left(y_k^2 + y_l^2 - y_i^2\right) - y_j^2 \right] \\ D_3 &= \frac{1}{30} y_j^3 \left[5\left(y_i^2 + y_k^2 + y_l^2\right) - y_j^2 \right] \end{aligned}$$

- $y_i + y_j < y_k + y_l$ and $y_i + y_l < y_j + y_k$:

$$\begin{aligned} D_1 &= \frac{1}{2}(y_i + y_j + y_l - y_k) \\ D_2 &= -\frac{1}{12}\left[(y_i + y_j)\left\{ (y_i + y_j)^2 - 3\left(y_k^2 + y_l^2\right) \right\} + 2\left(y_k^3 - y_l^3\right) \right] \\ D_3 &= \frac{1}{60}\left[y_k^5 - y_i^5 - y_j^5 - y_l^5 + 5\left(-y_k^3 y_l^2 + y_k^2 y_l^3 - y_k^3 y_i^2 + y_k^2 y_i^3 \right.\right. \\ &\qquad \left.\left. - y_k^3 y_j^2 + y_k^2 y_j^3 + y_l^3 y_i^2 + y_l^2 y_i^3 + y_l^3 y_j^2 + y_l^2 y_j^3 + y_i^3 y_j^2 + y_i^2 y_j^3 \right) \right] \end{aligned}$$

Going back to the collision integral, the same trick as before can be applied to the delta function of energies, which then gives:

$$I_{\text{coll}} = \frac{S}{64\pi^3 g\widetilde{E_1} y_1 a^5} \int \mathrm{d}y_2 \mathrm{d}y_3 \frac{y_2 y_3}{\widetilde{E_2}\widetilde{E_3}} \mathscr{D}(Y_1, Y_2, Y_3, Y_4) \cdot \\ \cdot \theta\left(\left(s_1\widetilde{E_1} + s_2\widetilde{E_2} + s_3\widetilde{E_3}\right)^2 - a^2 m_4^2\right) (F[f])\Big|_{y_4 = y_4^*} \quad , \tag{B.26}$$

with $y_4^* = \sqrt{\left(s_1\widetilde{E_1} + s_2\widetilde{E_2} + s_3\widetilde{E_3}\right)^2 - a^2 m_4^2}$.

B.2.2 Case $y_1 = 0$

$$I_{\text{coll}} = \frac{S}{64\pi^3 g a m_1} \frac{1}{a^5} \int \frac{\mathrm{d}y_2 \mathrm{d}y_3 \mathrm{d}y_4 y_2 y_3 y_4}{\widetilde{E_2}\widetilde{E_3}\widetilde{E_4}} F[f] \delta\left(s_1 a m_1 + s_2\widetilde{E_2} + s_3\widetilde{E_3} + s_4\widetilde{E_4}\right) \cdot \\ \cdot \mathscr{B}(Y_1, Y_2, Y_3, Y_4) \, , \tag{B.27}$$

with

$$\begin{aligned} \mathscr{B}(Y_1, Y_2, Y_3, Y_4) &= \frac{y_2 y_3 y_4}{64\pi^5} \int \mathrm{d}\Omega_2 \mathrm{d}\Omega_3 \mathrm{d}\Omega_4 \, |\mathscr{M}|^2 \, |\delta^3(s_2 \mathbf{y_2} + s_3 \mathbf{y_3} + s_4 \mathbf{y_4}) \\ &= \frac{y_2 y_3 y_4}{64\pi^5} \int \mathrm{d}\lambda \lambda^2 \mathrm{d}\Omega_\lambda \int \mathrm{d}\theta_2 \mathrm{d}\phi_2 \sin\theta_2 e^{i s_2 y_2 \lambda \cos\theta_2} \cdot \\ &\cdot \int \mathrm{d}\theta_3 \mathrm{d}\phi_3 \sin\theta_3 e^{i s_3 y_3 \lambda \cos\theta_3} \int \mathrm{d}\theta_4 \mathrm{d}\phi_4 \sin\theta_4 e^{i s_4 y_4 \lambda \cos\theta_4} \cdot \\ &\cdot \sum_{i \neq j \neq k \neq l} \left[K_1 \left(\widetilde{E_i}\widetilde{E_j} - y_i y_j \cos\theta_i \cos\theta_j\right) \cdot \left(\widetilde{E_k}\widetilde{E_l} - y_k y_l \cos\theta_k \cos\theta_l\right) + \right. \\ &\left. + K_2 \, a^2 m_i m_j \left(\widetilde{E_k}\widetilde{E_l} - y_k y_l \cos\theta_k \cos\theta_l\right)\right] \end{aligned} \tag{B.28}$$

Consider the case that $i = 1$ in one of the terms of $|\mathscr{M}|^2$. Then the $\mathscr{B}-$function can be written as:

$$\begin{aligned} \mathscr{B}_{i=1}(Y_1, Y_2, Y_3, Y_4) &= \frac{y_2 y_3 y_4}{64\pi^5} 4\pi \int \mathrm{d}\lambda \lambda^2 \sum_{j \neq k \neq l} \int \mathrm{d}\theta_j \mathrm{d}\phi_j \sin\theta_j e^{i s_j y_j \lambda \cos\theta_j} \cdot \\ &\cdot \int \mathrm{d}\theta_k \mathrm{d}\phi_k \sin\theta_k e^{i s_k y_k \lambda \cos\theta_k} \int \mathrm{d}\theta_l \mathrm{d}\phi_l \sin\theta_l e^{i s_l y_l \lambda \cos\theta_l} \cdot \\ &\cdot \left[K_1 a m_1 \widetilde{E_j} \cdot \left(\widetilde{E_k}\widetilde{E_l} - y_k y_l \cos\theta_k \cos\theta_l\right) + \right. \\ &\left. + K_2 \, a^2 m_1 m_j \left(\widetilde{E_k}\widetilde{E_l} - y_k y_l \cos\theta_k \cos\theta_l\right)\right] \end{aligned} \tag{B.29}$$

$$\mathscr{B}_{i=1}(Y_1,Y_2,Y_3,Y_4) = K_1 a m_1 \sum_{j\neq k\neq l} \left[\widetilde{E_j}\widetilde{E_k}\widetilde{E_l} B_1\left(y_j,y_k,y_l\right) + \widetilde{E_j} B_2\left(y_j,y_k,y_l\right)\right] + \\ + K_2 a m_1 \sum_{j\neq k\neq l} a m_j \left[\widetilde{E_k}\widetilde{E_l} B_1\left(y_j,y_k,y_l\right) + B_2\left(y_j,y_k,y_l\right)\right], \quad \text{(B.30)}$$

with $B_1\left(y_j,y_k,y_l\right)$ given by Eq. (B.9) and

$$B_2\left(y_j,y_k,y_l\right) = s_k s_l \frac{4y_k y_l}{\pi}\int \frac{\mathrm{d}\lambda}{\lambda}\sin(y_j\lambda)\left[\cos(y_k\lambda) - \frac{\sin(y_k\lambda)}{y_k\lambda}\right]\left[\cos(y_l\lambda) - \frac{\sin(y_l\lambda)}{y_l\lambda}\right] \\ = \begin{cases} \frac{1}{2}\left[y_k^2 + y_l^2 - y_j^2\right], & y_j + y_k \geq y_l \;\&\; y_j + y_l \geq y_k \;\&\; y_k + y_l \geq y_j \\ 0, \quad \text{otherwise} \end{cases} \quad \text{(B.31)}$$

This procedure can be done for all the other terms in $|\mathscr{M}|^2$. If $j = 1$, the result is the same, but with $i \leftrightarrow j$. Note that if $k = 1$ or $l = 1$, there is no B_2-term in the part with K_2. The collision integral then becomes

$$I_{\text{coll}} = \frac{S}{64\pi^3 g m_1 a^6}\int \mathrm{d}y_2\mathrm{d}y_3 \frac{y_2 y_3}{\widetilde{E_2}\widetilde{E_3}}\mathscr{B}(Y_1,Y_2,Y_3,Y_4)\cdot \\ \cdot\theta\left(\left(\left(s_1 \hat{a} m_1 + s_2\widetilde{E_2} + s_3\widetilde{E_3}\right)^2 - a^2 m_4^2\right)(F[f])\right|_{y_4 = y_4^*}, \quad \text{(B.32)}$$

with $y_4^* = \sqrt{\left(s_1 a m_1 + s_2\widetilde{E_2} + s_3\widetilde{E_3}\right)^2 - a^2 m_4^2}$.

APPENDIX C

TEMPERATURE EVOLUTION

Consider a plasma in an expanding universe consisting of four particle species, one out of each category in Section 2.2. For example, the four species here are photons, electrons, active neutrinos and HNLs. The addition of other species (e.g. muons) will then follow a similar procedure. In what follows: $\widetilde{T} = aT$, $\widetilde{E} = aE$. The total energy density and total pressure in comoving coordinates are given by

$$\rho_{\text{tot}} = \rho_\gamma + \rho_e + \rho_\nu + \rho_N \qquad P_{\text{tot}} = P_\gamma + P_e + P_\nu + P_N$$

$$\rho_\gamma = g_\gamma \frac{\pi^2}{30} \frac{1}{a^4} \widetilde{T}^4 \qquad P_\gamma = \frac{1}{3}\rho_\gamma$$

$$\rho_e = \frac{g_e}{2\pi^2} \frac{1}{a^4} \int \mathrm{d}y\, y^2 \frac{\widetilde{E_e}}{e^{\frac{1}{\widetilde{T}}\widetilde{E_e}} + 1} \qquad P_e = \frac{g_e}{6\pi^2} \frac{1}{a^4} \int \mathrm{d}y \frac{y^4}{\widetilde{E_e}} \frac{1}{e^{\frac{1}{\widetilde{T}}\widetilde{E_e}} + 1}$$

$$\rho_\nu = \frac{g_\nu}{2\pi^2} \frac{1}{a^4} \int \mathrm{d}y\, y^3 f_\nu \qquad P_\nu = \frac{1}{3}\rho_\nu$$

$$\rho_N = \frac{g_N}{2\pi^2} \frac{1}{a^4} \int \mathrm{d}y\, y^2 \sqrt{y^2 + a^2 m_N^2} f_N \qquad P_N = \frac{g_N}{6\pi^2} \frac{1}{a^4} \int \mathrm{d}y \frac{y^4}{\widetilde{E_N}} f_N$$

The energy conservation law (Eq. 2.3) in the variables considered here is

$$\frac{\mathrm{d}\rho_{\text{tot}}}{\mathrm{d}\ln a} \frac{\mathrm{d}\ln a}{\mathrm{d}t} + 3H\left(\rho_{\text{tot}} + P_{\text{tot}}\right) = 0 \Longrightarrow \frac{\mathrm{d}\rho_{\text{tot}}}{\mathrm{d}\ln a} + 3\left(\rho_{\text{tot}} + P_{\text{tot}}\right) = 0$$

Taking derivatives:

$$\frac{\mathrm{d}\rho_\gamma}{\mathrm{d}\ln a} = g_\gamma \frac{\pi^2}{30}\left(-4\frac{1}{a^4}\widetilde{T}^4 + 4\frac{1}{a^4}\widetilde{T}^3\frac{\mathrm{d}\widetilde{T}}{\mathrm{d}\ln a}\right) = -4\rho_\gamma + 4\frac{\rho_\gamma}{\widetilde{T}}\frac{\mathrm{d}\widetilde{T}}{\mathrm{d}\ln a}$$

$$\frac{\mathrm{d}\rho_e}{\mathrm{d}\ln a} = -4\rho_e + \frac{g_e}{2\pi^2}\frac{1}{a^4}\int \mathrm{d}y y^2 \left[\frac{\left(e^{\frac{1}{\widetilde{T}}\widetilde{E_e}}+1\right)\frac{a^2m_e^2}{\widetilde{E_e}} - \widetilde{E_e}e^{\frac{1}{\widetilde{T}}\widetilde{E_e}}\left(\frac{a^2m_e^2}{\widetilde{T}\widetilde{E_e}} - \frac{\widetilde{E_e}}{\widetilde{T}^2}\frac{\mathrm{d}\widetilde{T}}{\mathrm{d}\ln a}\right)}{\left(e^{\frac{1}{\widetilde{T}}\widetilde{E_e}}+1\right)^2}\right]$$

$$= -4\rho_e + \frac{g_e}{2\pi}\frac{1}{a^4}\int \mathrm{d}y y^2 \left[\frac{a^2m_e^2}{\widetilde{E_e}}\frac{1}{e^{\frac{1}{\widetilde{T}}\widetilde{E_e}}+1} - \left(\frac{a^2m_e^2}{\widetilde{T}} - \frac{\left(\widetilde{E_e}\right)^2}{\widetilde{T}^2}\frac{\mathrm{d}\widetilde{T}}{\mathrm{d}\ln a}\right)\frac{e^{\frac{1}{\widetilde{T}}\widetilde{E_e}}}{\left(e^{\frac{1}{\widetilde{T}}\widetilde{E_e}}+1\right)^2}\right]$$

$$\frac{\mathrm{d}\rho_\nu}{\mathrm{d}\ln a} = -4\rho_\nu + \frac{g_\nu}{2\pi^2}\frac{1}{a^4}\int \mathrm{d}y y^3 \frac{\mathrm{d}f_\nu}{\mathrm{d}\ln a} = -4\rho_\nu + \frac{g_\nu}{2\pi^2}\frac{1}{a^4}\int \mathrm{d}y y^3 \frac{1}{H} I_\nu$$

$$\frac{\mathrm{d}\rho_N}{\mathrm{d}\ln a} = -4\rho_N + \frac{g_N}{2\pi^2}\frac{1}{a^4}\int \mathrm{d}y y^2 \left[\frac{a^2m_N^2}{\widetilde{E_N}} + \widetilde{E_N}\frac{\mathrm{d}f_N}{\mathrm{d}\ln a}\right]$$

$$= -4\rho_N + \frac{g_N}{2\pi^2}\frac{1}{a^4}\int \mathrm{d}y y^2 \left[\frac{a^2m_N^2}{\widetilde{E_N}} + \widetilde{E_N}\frac{1}{H} I_N\right]$$

Doing the individual species first:

$$\frac{\mathrm{d}\rho_\gamma}{\mathrm{d}\ln a} + 3\left(\rho_\gamma + P_\gamma\right) = 4\frac{\rho_\gamma}{\widetilde{T}}\frac{\mathrm{d}\widetilde{T}}{\mathrm{d}\ln a}$$

$$\frac{\mathrm{d}\rho_e}{\mathrm{d}\ln a} + 3\left(\rho_e + P_e\right) = \frac{1}{a^4}\left[-\frac{a^2m_e^2}{\widetilde{T}}R_1 + \frac{1}{\widetilde{T}^2}\left\{R_2 + a^2m_e^2R_1\right\}\frac{\mathrm{d}\widetilde{T}}{\mathrm{d}\ln a}\right]$$

$$\frac{\mathrm{d}\rho_\nu}{\mathrm{d}\ln a} + 3\left(\rho_\nu + P_\nu\right) = \frac{g_\nu}{2\pi^2}\frac{1}{a^4}\int \mathrm{d}y y^3 \frac{1}{H} I_\nu$$

$$\frac{\mathrm{d}\rho_N}{\mathrm{d}\ln a} + 3\left(\rho_N + P_N\right) = \frac{g_N}{2\pi^2}\frac{1}{a^4}\int \mathrm{d}y y^2 \widetilde{E_N}\frac{1}{H} I_N\,,$$

with

$$R_1 = \frac{g_e}{2\pi^2}\int \mathrm{d}y y^2 \frac{e^{\frac{\widetilde{E_e}}{\widetilde{T}}}}{\left(e^{\frac{\widetilde{E_e}}{\widetilde{T}}}+1\right)^2}$$

$$R_2 = \frac{g_e}{2\pi^2}\int \mathrm{d}y y^4 \frac{e^{\frac{\widetilde{E_e}}{\widetilde{T}}}}{\left(e^{\frac{\widetilde{E_e}}{\widetilde{T}}}+1\right)^2}$$

Adding all these terms together and solving for the temperature change gives:

$$\frac{\mathrm{d}\widetilde{T}}{\mathrm{d}\ln a} = \frac{\frac{a^2m_e^2}{\widetilde{T}}R_1 - \frac{g_\nu}{2\pi^2}\int \mathrm{d}y y^3 \frac{1}{H} I_\nu - \frac{g_N}{2\pi^2}\int \mathrm{d}y y^2 \widetilde{E_N}\frac{1}{H} I_N}{\frac{2\pi^2 g_\gamma}{15}\widetilde{T}^3 + \frac{1}{\widetilde{T}^2}R_2 + \frac{a^2m_e^2}{\widetilde{T}^2}R_1} \tag{C.1}$$

APPENDIX D

NEUTRINO OSCILLATIONS

The active neutrinos in the flavour basis $|\nu_\alpha\rangle$ are related to the mass basis $|\nu_i\rangle$ via

$$\begin{pmatrix} \nu_e \\ \nu_\mu \\ \nu_\tau \end{pmatrix} = V_{\text{PMNS}} \begin{pmatrix} \nu_1 \\ \nu_2 \\ \nu_3 \end{pmatrix} \quad ,$$

with V_{PMNS} the non-diagonal Pontecorvo-Maki-Nakagawa-Sakata matrix, given by

$$V_{\text{PMNS}} = \begin{pmatrix} 1 & 0 & 0 \\ 0 & c_{23} & s_{23} \\ 0 & -s_{23} & c_{23} \end{pmatrix} \begin{pmatrix} c_{13} & 0 & s_{13} \\ 0 & e^{i\phi} & 0 \\ -s_{13} & 0 & c_{13} \end{pmatrix} \begin{pmatrix} c_{12} & s_{12} & 0 \\ -s_{12} & c_{12} & 0 \\ 0 & 0 & 1 \end{pmatrix}$$

Here $c_{ij} = \cos\theta_{ij}$, $s_{ij} = \sin\theta_{ij}$ and θ_{ij} are the active neutrino mixing angles. Characteristic time scale of oscillations between two flavours consisting of mass eigenstates $|\nu_i\rangle$ and $|\nu_j\rangle$ for neutrinos with energy E is [29]

$$\tau_{ij} \sim \frac{4\pi E}{\left|m_i^2 - m_j^2\right|} \sim 8 \cdot 10^{-6} \text{ s } \frac{E}{\text{MeV}} \frac{10^{-3} \text{ eV}^2}{\left|m_i^2 - m_j^2\right|}$$

Assuming propagation in vacuum with $E \approx \pi T$ and using the measured mass differences $|m_2^2 - m_1^2| \approx 7.6 \cdot 10^{-5}$ eV^2 and $\left|m_3^1 - m_1^2\right| \approx 2.5 \cdot 10^{-3}$ eV^2 [26], the time scales are

$$\tau_{12} \approx 3 \cdot 10^{-4}\ \mathrm{s}\ \frac{T}{\mathrm{MeV}}$$
$$\tau_{13} \approx 10^{-5}\ \mathrm{s}\ \frac{T}{\mathrm{MeV}}$$

The Hubble time at temperature of 1 MeV and for $g_* = 11$ is given by

$$\tau_{\mathrm{H}} = \frac{M_{\mathrm{pl}}}{1.66\sqrt{g_*}}\frac{1}{T^2} \approx 1.4\ \mathrm{s}\ \left(\frac{\mathrm{MeV}}{T}\right)^2$$

The characteristic oscillation time scales τ_{12} and τ_{13} are much smaller than the Hubble time. At temperatures $T \approx 1$ MeV, weak reaction rates are of the same order as the Hubble rate. Therefore, active neutrinos will oscillate many times between subsequent reactions that involve them. In reality, active neutrinos are created in wave packets that consist of superposition of states, each of which has its own definite momentum and own characteristic oscillation time as shown above. Between two reactions these states will oscillate many times and the phases of the superpositions of these states will not be correlated. Therefore, it is possible to describe this oscillation phenomenon by means of time-averaged transition probabilities $P_{\alpha\beta}$, given by [29]

$$P_{ee} = 1 - \frac{1}{2}\left[\sin^2(2\theta_{13}) + \cos^4(\theta_{13})\sin^2(2\theta_{12})\right]$$
$$P_{e\mu} = P_{\mu e} = \frac{1}{2}\cos^2(\theta_{13})\sin^2(2\theta_{12})$$
$$P_{e\tau} = P_{\tau e} = \sin^2(\theta_{13})\cos^2(\theta_{13})\left[2 - \frac{1}{2}\sin^2(2\theta_{12})\right]$$
$$P_{\mu\mu} = 1 - \frac{1}{2}\sin^2(2\theta_{12})$$
$$P_{\mu\tau} = P_{\tau\mu} = \frac{1}{2}\sin^2(\theta_{13})\sin^2(2\theta_{12})$$
$$P_{\tau\tau} = 1 - \sin^2(\theta_{13})\left[2\cos^2(\theta_{13}) + \frac{1}{2}\sin^2(\theta_{13})\sin^2(2\theta_{12})\right]$$

BIBLIOGRAPHY

[1] Y. AOKI, S. BORSANYI, S. DURR, Z. FODOR ET AL., *The QCD transition temperature: results with physical masses in the continuum limit II.*, JHEP **06** (2009) 088, [0903.4155].

[2] T. ASAKA, S. BLANCHET AND M. SHAPOSHNIKOV, *The nuMSM, dark matter and neutrino masses*, Phys. Lett. **B631** (2005) 151–156, [0503065].

[3] T. ASAKA AND M. SHAPOSHNIKOV, *The nuMSM, dark matter and baryon asymmetry of the universe*, Phys. Lett. **B620** (2005) 17–26, [0505013].

[4] E. AVER, K. A. OLIVE AND E. D. SKILLMAN, *An MCMC determination of the primordial helium abundance*, JCAP **1204** (2012) 004, [1112.3713].

[5] R. BARBIERI AND A. DOLGOV, *Bounds on Sterile-neutrinos from Nucleosynthesis*, Phys. Lett. **B237** (1990) 440–445.

[6] K. BONDARENKO, A. BOYARSKY, D. GORBUNOV AND O. RUCHAYSKIY, *Phenomenology of GeV-scale Heavy Neutral Leptons*, arXiv preprint (2018) , [1805.08567].

[7] A. BOYARSKY, O. RUCHAYSKIY AND M. SHAPOSHNIKOV, *The Role of sterile neutrinos in cosmology and astrophysics*, Ann. Rev. Nucl. Part. Sci. **59** (2009) 191–214, [0901.0011].

[8] J. COLLINS, *Foundations of perturbative QCD*, Cambridge University Press, Cambridge, UK, 2013.

[9] R. H. CYBURT, B. D. FIELDS, K. A. OLIVE AND T.-H. YEH, *Big Bang Nucleosynthesis: 2015*, Rev. Mod. Phys. **88** (2016) 015004, [1505.01076].

[10] A. D. DOLGOV, S. H. HANSEN, G. RAFFELT AND D. V. SEMIKOZ, *Cosmological and astrophysical bounds on a heavy sterile neutrino and the KARMEN anomaly*, Nucl. Phys. **B580** (2000) 331–351, [0002223].

[11] A. D. DOLGOV, S. H. HANSEN, G. RAFFELT AND D. V. SEMIKOZ, *Heavy sterile neutrinos: Bounds from big bang nucleosynthesis and SN1987A*, Nucl. Phys. **B590** (2000) 562–574, [0008138].

[12] A. D. DOLGOV, S. H. HANSEN AND D. V. SEMIKOZ, *Impact of massive tau neutrinos on primordial nucleosynthesis. Exact calculations*, Nucl. Phys. **B524** (1998) 621–638, [9712284].

[13] A. D. DOLGOV AND D. P. KIRILOVA, *Nonequilibrium Decays of Light Particles and the Primordial Nucleosynthesis*, Int. J. Mod. Phys. **A3** (1988) 267.

[14] G. M. FULLER, C. T. KISHIMOTO AND A. KUSENKO, *Heavy sterile neutrinos, entropy and relativistic energy production, and the relic neutrino background*, arXiv preprint (2011) , [1110.6479].

[15] J. GHIGLIERI AND M. LAINE, *Neutrino dynamics below the electroweak crossover*, JCAP **1607** (2016) 015, [1605.07720].

[16] I. GHISOIU AND M. LAINE, *Right-handed neutrino production rate at $T > 160$ GeV*, JCAP **1412** (2014) 032, [1411.1765].

[17] S. HANNESTAD, *What is the lowest possible reheating temperature?*, Phys. Rev. **D70** (2004) 043506, [0403291].

[18] M. KAWASAKI ET AL., *Big bang nucleosynthesis constraints on the tau-neutrino mass*, Nucl. Phys. **B419** (1994) 105–128.

[19] M. KAWASAKI, K. KOHRI AND N. SUGIYAMA, *MeV scale reheating temperature and thermalization of neutrino background*, Phys. Rev. **D62** (2000) 023506, [0002127].

[20] E. W. KOLB AND M. S. TURNER, *The Early Universe*, Addison-Wesley, Redwood City, USA, 1990.

[21] G. MANGANO, G. MIELE, S. PASTOR, T. PINTO ET AL., *Relic neutrino decoupling including flavor oscillations*, Nucl. Phys. **B729** (2005) 221–234, [0506164].

[22] V. MUKHANOV, *Physical Foundations of Cosmology*, Cambridge University Press, Cambridge, UK, 2005.

[23] D. NOTZOLD AND G. RAFFELT, *Neutrino Dispersion at Finite Temperature and Density*, Nucl. Phys. **B307** (1988) 924–936.

[24] C. PATRIGNANI ET AL., *Review of Particle Physics*, Chin. Phys. **C40** (2016) 100001.

[25] O. RUCHAYSKIY AND A. IVASHKO, *Restrictions on the lifetime of sterile neutrinos from primordial nucleosynthesis*, JCAP **1210** (2012) 014, [1202.2841].

[26] T. SCHWETZ, M. TORTOLA AND J. W. F. VALLE, *Where we are on θ_{13}: addendum to 'Global neutrino data and recent reactor fluxes: status of three-flavour oscillation parameters'*, New J. Phys. **13** (2011) 109401, [1108.1376].

[27] M. SHAPOSHNIKOV, *The nuMSM, leptonic asymmetries, and properties of singlet fermions*, JHEP **08** (2008) 008, [0804.4542].

[28] C. J. SMITH, G. M. FULLER AND M. S. SMITH, *Big Bang Nucleosynthesis with Independent Neutrino Distribution Functions*, Phys. Rev. **D79** (2009) 105001, [0812.1253].

[29] A. STRUMIA AND F. VISSANI, *Neutrino masses and mixings and...*, arXiv preprint (2006) , [0606054].